http://dx.doi.org/10.5935/0103-5053.20150011

J. Braz. Chem. Soc., Vol. 26, No. 3, 562-571, 2015.
Printed in Brazil - ©2015 Sociedade Brasileira de Química
0103 - 5053 $6.00+0.00

Article

Quinolines by Three-Component Reaction: Synthesis and Photophysical Studies

Eric S. Sales,[a] Juliana M. F. M. Schneider,[a] Marcos J. L. Santos,[a] Adailton J. Bortoluzzi,[b] Daniel R. Cardoso,[c] Willy G. Santos,[c] and Aloir A. Merlo*,[a]*

[a]*Instituto de Química, Universidade Federal do Rio Grande do Sul (UFRGS), 90040-060 Porto Alegre-RS, Brazil*

[b]*Departamento de Química, Universidade Federal de Santa Catarina(UFSC), 88040-900 Florianópolis-SC, Brazil*

[c]*Chemistry Institute of São Carlos, Universidade de São Paulo (USP), 13566-590 São Carlos-SP, Brazil*

The synthesis of five quinolines 8-octyloxy-4-[4-(octyloxy)phenyl]quinoline and 6-alkoxy-2-(4-alkoxyphenyl)-4-[(4-octyloxy)aryl]quinolines are described by three-component coupling reaction mediated by Lewis acid $FeCl_3$ and $Yb(OTf)_3$. 4-*n*-octyloxybenzaldehyde, anisaldehyde, 4-*n*-octyloxyaniline *p*-anisidine, and 1-ethynyl-4-heptyloxybenzene, 1-ethynyl-4-octyloxybenzene and 2-ethynyl-6-heptyloxynaphthalene are the reagents in this protocol. A Yb^{3+} catalyst resulted in higher yields of quinolines than Fe^{3+}. Polarizing optical microscopy (POM) revealed that none of the quinolines were liquid crystals, even the more anisotropic. UV-Vis measurements of one of the quinolines in polar solvent show two absorption bands at 280 and 350 nm related to π,π* and n,π* transitions. No changes were observed to lower-energy absorption band ($\varepsilon < 10^4$ mol L^{-1} cm^{-1}) related to n,π* transition. A laser flash photolysis study for one of the quinolines relates a main transient band at 450 nm with a lifetime of 2.6 μs in ethanol, which is completely quenched in the presence of oxygen. This transient band was assigned to triplet-triplet absorption of one of the quinolines, which is semi-oxidised in the presence of phenol. Radiative rate constants have been determined along singlet and triplet excited state energies (3.39 and 3.10 eV, respectively). The chemical structure of one of the quinolines was also unequivocally confirmed by single-crystal X-ray analysis.

Keywords: quinolines, three-component synthesis, single-crystal resolution, photophysics, flash photolysis

Introduction

Quinolines are present in many pharmacologically active natural compounds. The simplest structure is the 1-azanaphthalene named quinoline itself, which was prepared by Friedländer in 1882 through the condensation of *o*-aminobenzaldehyde with acetaldehyde in the presence of sodium hydroxide.[1] Quinolines display a broad spectrum of application in medicine, such as antiseptic, antimalarial, and as fungicides and antibiotics. Chloroquine is the most well-known drug, and has been applied for the control and treatment of malaria for many decades.[2-4] Some quinolines such as chloroquine, amodiaquine and quinine can be safely used during pregnancy.[5] Primaquine, however, another drug used in the treatment of malaria, should not be used during pregnancy.[6]

The biological activity of chloroquine was evaluated through fluorescence quenching studies developed by Naal *et al*.[7] Their findings provide information about the chloroquine-micellar surface interactions in water and their ability to cross biological membranes in order to accumulate inside lysosomes.

The combination of quinoline ring and styryl moiety resulted in a small and powerful luminescent molecular material, which presents pronounced fluorescence and noticeable nonlinear responses to be exploited in protochromic ON-OFF-ON effects.[8] In addition, small fluorescent molecules can be applied for the detection of fibrillar aggregates by binding to the fibril and changing its fluorescence properties by absorbing and emitting light

*e-mail: aloir.merlo@ufrgs.br, willy_glen@yahoo.com.br

in the far red/near-infrared (NIR) region (ca. 600-800 nm). Under this circumstance, tissue scattering and absorption is lowest. Most particularly, they are able to cross the blood-brain barrier due to their small molecular size.[9,10]

Industrial applications of quinolines include use as dyes, preservatives and ligands to metal complexes, and have strong impact in luminescence chemistry.[11] Multi-component reactions are a useful tool to synthesize molecules from simple to complex architectures in a way that their chemical and pharmaceutical properties can be explored, making quinolines important in pharmacology and functional material chemistry.[12]

Quinolines are fluorescent molecules with good electron acceptance in biological media and in devices. The potential redox of simple quinolines is a reversible process. However, the potential redox, and the absorption and spectral emission properties of quinoline derivatives can be tailored by appropriate substitution in the quinoline ring or/and in the peripheral aryl groups.[13]

We here report our results involving the synthesis and characterisation of new quinolines synthesised by three-component reaction between aldehyde, amine and alkyne under Lewis catalyst $FeCl_3$ and $Yb(OTf)_3$. Ground-state and excited-stated dynamics analysis are discussed for one quinoline synthesised in this work along with electrochemical data. These results will be exploited in the future, in the preparation and utilisation of new iridium complexes in the field of organic-light emitting diodes (OLEDs) and metal-complex liquid crystals (MCLC).[13]

Results and Discussion

Synthesis

The preparation of key intermediates for the three-component reaction of the quinolines **8a**-**e** is described in Scheme 1. Aldehyde **2a** was obtained by alkylation reaction of **1**, in nearly quantitative yield.[14] Amines **4a**-**b** were prepared in two steps: alkylation reaction followed by reduction of the nitro group to the amine group by means of hydrogenolysis reaction (H_2/Pd/C in MeOH).[15] Aldehydes **2b** and **2c** and amine **4c** are commercial chemicals. Alternatively, they can be prepared using the condition reaction described by Vogel[16] and Markiewicz *et al.*[16] Alkynes **7a**-**b** were synthesised in three steps, starting with **5** by alkylation reaction, followed by Sonogashira cross-coupling reaction and acetone release in the basic medium to give **7a** and **7b** in good yields.[17] Alkyne **7c**[17] was made similarly to **7a**-**b** from 6-bromo-2-napthol.

Since the preparation of the intermediates **2a**, **4a**, **7a**-**b** was accomplished, metal-catalysed three-component

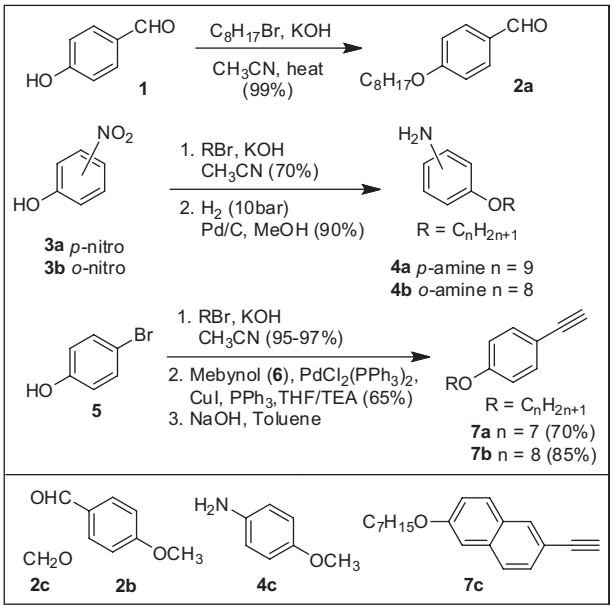

Scheme 1. Preparation of key intermediates **2a**, **4a** and **7a**-**b**.

coupling[4] was performed as outlined in Scheme 2. Two Lewis acids were tested: $FeCl_3$ and $Yb(OTf)_3$ as a catalyst of three-component coupling. $FeCl_3$ was chosen due to its low price, non-toxicity, and environmental friendly characteristics.[18] Despite the attributes mentioned above, the approach using a three-component reaction with Fe(III) resulted in poor yield and reproducibility. Very low yields were obtained for **8a** (12%), **8b** (15%) and **8c** (13%) using $FeCl_3$. When the catalyst ratio was increased to 20 mol%, the yield of **8b** rose to 40%. Previous work by Furukawa[19] showed that the Yb(III) triflate is an effective catalyst to prepare 2-arylquinolines. Following the procedure described by Furukawa,[19] quinolines **8c** and **8d** were obtained in 40% and 60%, by using Yb(III) triflate as a catalyst. The ratio of catalyst (mol%), yields (%) and melting point (°C) for quinolines **8a**-**e** are shown in Table 1.

The mechanism for the formation of the quinoline derivatives is generally accepted as activation on both processes of imine addition and cyclization. The double and triple bond of both imine group and alkyne could be activated by a Lewis acid such as Au(III),[20] Fe(III)[21] and Yb(III).[22] The complexation effect promotes the formation of propargylamine intermediate A,[23] which undergoes an intramolecular hydroarylation[24] to give another intermediate dihydroquinoline B. Propargylamine A is generally isolated when aliphatic amines are used. In the present study, no attempt to detect or to isolate intermediate A was made. Dihydroquinolines could then be further oxidized by O_2[25] to afford quinoline products **8a**-**e**. In summary, this one-pot reaction undergoes domino imine formation, imine addition, cyclization and an oxidation process.

Table 1. Lewis acid and yields (%) of quinolines **8a-e**

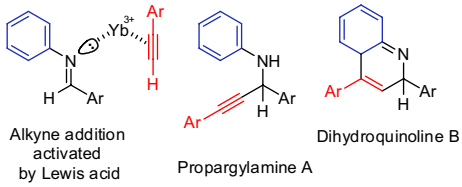

Quinoline	Lewis acid / (mol%)	Yield / %	Melting point / °C
8a	$FeCl_3$ (12)	12	68-70
8b	$FeCl_3$ (10)	15	85-86
	$FeCl_3$ (20)	40	
8c	$FeCl_3$ (10)	13	75-76
	$Yb(OTf)_3$ (10)	60	
8d	$Yb(OTf)_3$ (10)	40	87-88
8e	$Yb(OTf)_3$ (10)	36	67-68

The three-component protocol applied in this study allows us to prepare new quinolines, which are, of course, naturally anisotropic. The choice of amines, aldehydes and alkynes are crucial in order to reach the final anisometric-shape molecules. However, concerning phase transition, these new quinolines are not liquid crystals. According to polarising optical microscopy (POM) studies, no evidence of mesophases was observed. Upon heating or cooling, the quinolines pass directly from solid state to isotropic state or *vice versa*. Upon cooling, quinolines **8a-e** display a large hysteresis range and they recrystallize well below their melting point, while when left for a long time at room temperature, they recrystallize very slowly. A homeotropic film was also observed over a large area of the sample from the POM texture. Unfortunately, neither enantiotropic nor monotropic behaviour can be seen in those samples. Starting from simple quinoline **8a** and adding a second aryl group or lengthening the flexible alkyl chain were not enough for the generation of liquid crystal properties as exemplified by the more anisotropic quinoline **8e** one.

A particularly interesting feature of the single-crystal X-ray structure of **8e** is related to the pendant naphthyl group. It is twisted 65.2° from the plane of the quinoline unit. A flexible alkyl chain linked to this pendant aryl group is also randomly coiled, which indicates non-longer planarity of the molecule and a non-favourable molecular package. In fact, the absence of a mesophase for the quinolines **8a-e** can be attributed to the planarity and package structure. Although our efforts in preparation of the mono- and disubstituted arylquinolines liquid crystals as exemplified by **8a** and **8b-e** failed, we performed a photophysical study of donor-acceptor luminescent molecules derived from quinolines in this work.

The single crystal X-ray diffraction studies

The structural characterization of quinolines obtained by three component reaction was also established unequivocally by single crystal X-ray structure analysis of quinoline **8e** (Figure 1, top). The single crystal X-ray diffraction studies for **8e** were accomplished successfully, showing distinct conformation behaviour of alkylaryl groups linked to the quinoline moiety. The structure of **8e** shows that the phenyl group is almost coplanar, whereas the pendant naphthyl group is twisted compared to the plane of the quinoline unit. The torsion angle for N1-C1-C10-C11 is 7.30(17)° and for C4-C3-C24-C33 is 65.22(15)°. From this point of view, the electron migration is more pronounced through the phenyl-quinolinyl system than the naphtyl-quinolinyl system. The preference for non-coplanarity of the naphtyl group is due to a hydrogen atom at the C5 carbon atom where the free rotation around

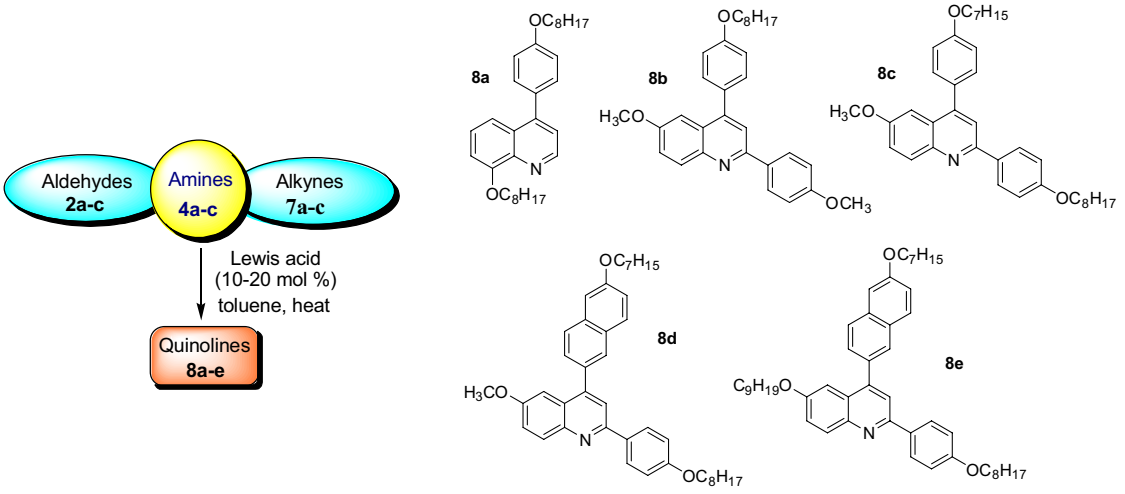

Scheme 2. Three-component synthesis of quinolines **8a-e**.

C3-C24 bond is hindered by a steric effect hydrogen atom. The conformational issue observed in this study has been also observed in kinetics studies of hydrolysis of acetoxy naphthoic acids.[26] To overcome this geometrical constraint, the bond length of the aryl group attached at the bay of the quinoline ring are slightly different. For instance, the bond length of C1-C10 is 1.4868(16) Å, while for C3-C24, the bond length value is longer by 0.0057 Å (1.4925(14) Å). Although the arrangement of the aryl groups at the bay of quinoline ring is quite different, the torsion angles to the three set of atoms namely C7-C6-O3-C41, C14-C13-O1-C16 and C30-C29-O2-C34 are 179.38(10)°, 177.72(11)° and 178.13(11)°, respectively. Thus, the first carbon atom of the alkyl chains is located on the same plane as the aryl and quinolinyl groups. The alkoxy chain connected to the C6 and C13 aromatic carbon atoms have an antiperiplanar arrangement for most carbon atoms including O1 and O3 oxygen atoms. However, the third alkoxy group connected to C29 aromatic carbon atom does not have an antiperiplanar arrangement for all saturated carbon atoms. They probably lost their conformational memory due to the twisted disposition of the naphthyl group to which they are bonded. The flexible alkyl chain linked to the pendant naphthyl group is randomly coiled. The disordered pendant group in **8e** aligns itself in an opposite direction, exhibiting alternate dispositions such as head-tail.

We suggest that the conformational behaviour observed in the crystal state may have an influence on the mesogenic behaviour as well as on the photophysical properties. The packing analysis shows neighbouring quinoline units are almost coplanar with respect to each other, with an average distance of 3.8 Å, exhibiting face-to-face π-stacking (Figure 1, bottom). The single crystal structure of quinoline **8e** provides a basis for elucidating the effect of solid-state morphology on their photophysics and liquid-crystalline properties. The absence of a mesophase, the glass-like appearance of the samples after heating/cooling cycles and UV-Vis absorption spectra profile are related to the molecular packing, as revealed by crystal structure of **8e**.

Ground-state and excited singlet-state: dependence on solvent and temperature

The UV-Vis absorption and fluorescence emission spectra of the quinolines **8a-e** are shown in Figures 2 and 3. The substitution of an aryl group affects the two absorption bands in different ways; in fact, the *p*-alcoxyaryl group in C_4 position of quinoline ring does not seem to greatly disturb the electronic UV-Vis spectrum of **8a**, while the *p*-alkoxyphenyl group in C_2 position induces the rise of the band at 290 nm, as observed for **8b-e** in Figure 2. The comparison between the UV-Vis spectra of quinoline and **8a** reveals similar patterns (optical behaviour) in the interval of wavelength of 270-330 nm.[27] Quinoline itself and quinoline **8a** have similar spectra, indicating that the aryl group in C_4 position does not change the chromophore characteristics. However, when an alkoxyaryl group is present in C_2 position, the quinolines **8b-e** absorption shows an intense band around 290 nm, which is not observed to **8a**. The quinolines **8a-e** have similar absorption at the 230-320 nm range, which is assigned to π,π transition that shifts to red in polar solvent (acetonitrile and ethanol) and is characterized by a large molar absorption coefficient. The n,π* transitions are observed as a shoulder in the

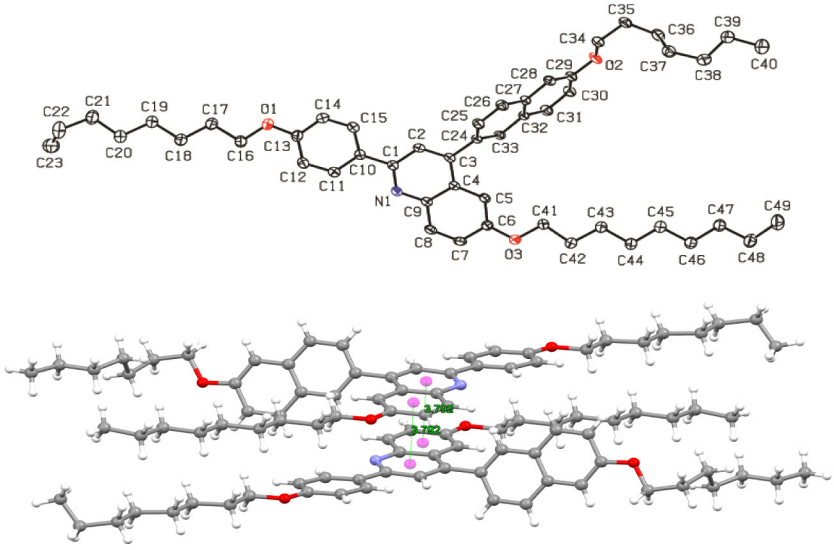

Figure 1. ORTEP plot of compound **8e** (top) and a view of partial packing of **8e** showing face-to-face π-stacking between neighbouring quinoline units (bottom, centroids are shown in magenta, see Supplementary Information (SI)).

320-450 nm range (ε ca. 10^3 mol^{-1} L cm^{-1}), which is not shifted in polar solvent, as shown in Figure 2.

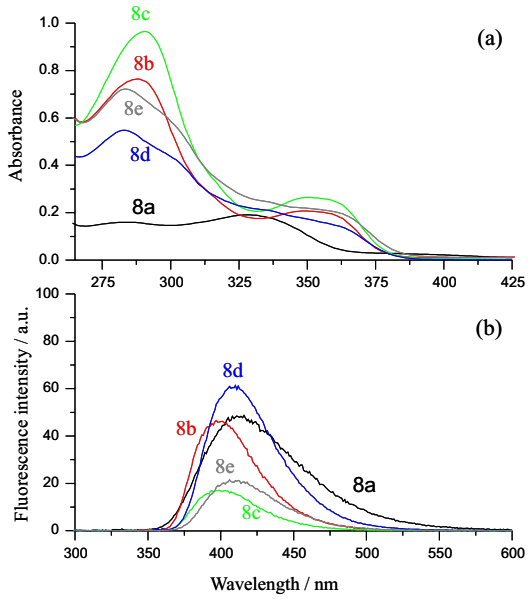

Figure 2. Absorption (a) and fluorescence (b) spectra of quinolines **8a**-**e** in dichloromethane (DCM); λ_{exc} = 350 nm.

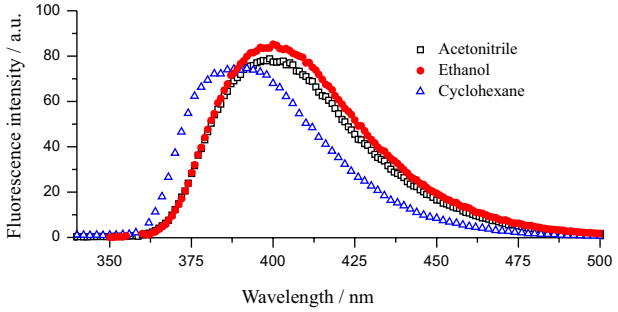

Figure 3. Emission spectra recorded to the quinoline **8b** in acetonitrile (□), ethanol (●) and cyclohexane (△). λ_{exc} = 350 nm.

In contrast with absorption, the solvent polarity affects the fluorescence properties of quinolines. The Stokes shift data, given by the difference between the maximum peak of normalised absorption and emission spectra, and the energy of the lowest singlet excited state, E_{S1}, which is estimated from the intersection of the normalised absorption and emission spectra, is observed in Table 3. No significant changes are observed on the Stokes shifts when replacing acetonitrile with ethanol. E_{S1} is independent of the solvent, with energy of 3.39 eV, discarding a hydrogen-bond interaction in the excited single-state. The compounds studied exhibit an overall increase of Stokes shift from non-polar to polar solvents mainly due to the combined effect of increasing the polarity of the medium and intramolecular charge transfer state (ICT). Other researchers relate the presence of the ICT state in quinoline molecules to the density functional theory and experimental studies.[28,29] The absorption spectrum of **8d** has an extinction coefficient of 1.4×10^4 mol^{-1} L cm^{-1} at 350 nm in ethanol. The fluorescence of quinoline **8d** in ethanol at 298 K and 77 K is shown in Figure 4, which is more intense at low temperature (77 K) with a maximum of 400 nm, indicating a relevant and competitive non-radiative process to deactivate the excited single-state.

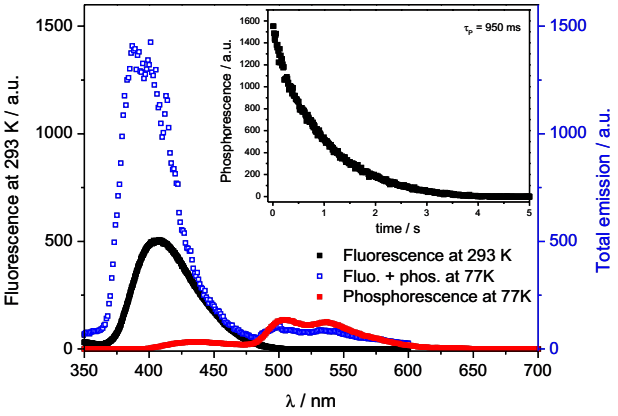

Figure 4. Fluorescence and phosphorescence emission (total emission) of **8d** in ethanol at 77 K (blue dots) and fluorescence emission at 293 K (black dots). Insert demonstrates the phosphorescence time decay at 77 K.

The quinoline derivatives **8a**-**e** present an emission band around 400 nm in polar solvent. The maximum absorption and emission wavelength and other photophysical properties of quinoline derivatives are shown in Table 2. Quinoline **8d** displays a phosphorescence emission at 77 K

Table 2. Photophysical properties of quinolines **8a**-**e** in DCM

Quinolines	λ_{MAX}^{abs} [a] / nm		λ_{MAX}^{em} [a] / nm	λ_{ST} / nm	ε × 10^3 / (mol^{-1} L cm^{-1})		ΔE[a] / eV		Φ_{FX} [b]
	π-π*	n-π*	n-π*		π-π*	n-π*	π-π*	n-π*	
8a	245	330	411	81	–	1.9	2.64	–	0.24
8b	288	350	398	48	51	1.7	3.02	2.49	0.22
8c	290	350	399	49	66	18	3.00	2.49	0.27
8d	282	347	409	62	41	14	3.08	2.51	0.25
8e	285	350	407	57	44	14	3.07	2.49	0.30

[a]Optical measurements condition: DCM, 298 K; [b]quinine sulphate 1 mol L^{-1} was used as fluorescent standard (Φ^o_F = 0.546, λ_{exc} = 337 nm).

in ethanol solution, showing clear vibrational resolution with three main bands at 440, 505 and 540 nm, which have the same time decay of 950 ms, close to that reported for other quinolines (0.5-1.5 s).[28] Phosphorescence properties and others photophysical characterisation can be found in Table 3. Figure 5 shows the transient species of **8d** obtained by laser pulse excitation at 355 nm in the absence of oxygen. Quinoline **8d** presents three transient absorption bands centred at 250 nm, 450 nm and 900 nm with the same time decay in ethanol. The lifetime decay of 2.6 μs was observed in all spectra, suggesting T-T character absorption.

Table 3. Photophysical properties of **8d**

Photophysical properties	Quinoline **8d**[a]
λ_{abs} / nm	355; 294; 280; 255; 225
λ_{em} / nm	397
λ_{phos} / nm	440; 503; 535
$<\tau_F>$ / ns	2.53
ϕ_F	0.22 (293 K); 0.40 (77 K)
k_F / s^{-1}	8.69×10^7 (293 K)
ϕ_P (77K)	0.03
τ_P (77K) / ms	950
$\lambda_{T\text{-}T\ max}$ / nm	450
$\tau_{T\text{-}T}$ / μs	2.60
E_{S1} / eV	3.39
E_{T1} / eV	3.10

[a]The underlined values are the absorption band used for fluorescence excitation and laser flash photolysis (LFP) excitation.

The shoulder observed in the absorption spectra in the 380 nm region with time decay of 6.8 μs is assigned to the semioxidized radical of the **8d** formed by self-quenching.

$$^3Q + Q_o \rightarrow Q^{\bullet+}_{s-ox} + Q^{\bullet-}_{s-red}$$

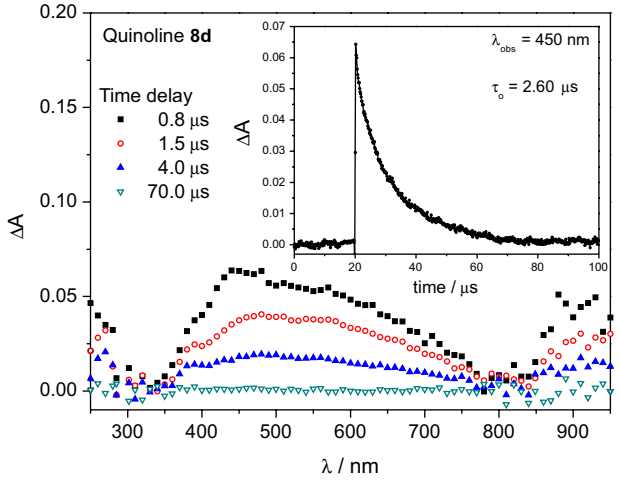

Figure 5. Transient spectra of **8d** in ethanol at different time delay. λ_{exc} = 355 nm at 12 mJ.

Quinoline **8d** can form a semi-oxidised radical specie ($Q^{\bullet+}$) at 350-450 nm and a semi-reduced form of quinoline ($Q^{\bullet-}$) at 740 nm by reaction with electron acceptor and electron donors molecules, respectively. Nedoloujko and Kiwi[30] relate the lifetime of semi-oxidized radical around 4 μs at 400 nm, comparable to **8d** specie at the same spectral range. No differences in the absorption spectra of **8d** were observed in methanol, ethanol, methylcyclohexane or acetonitrile as solvent, however, in aired solution, the T-T absorption of **8d** was totally quenched in ethanol. In the presence of a high concentration of phenol ($\times 10^{-4}$ mol L^{-1}), the triplet of **8d** is quenched, simultaneously with an increase of the absorption in 280-500 nm range. These absorptions can be ascribed to a semi-oxidized form of **8d**, formed by an electron transfer donation to phenol. Figure 6a shows the effect of phenol in the **8d** absorption spectra. In photolysis experiments, the reaction of dye triplets with phenols is very well-known and leads to the formation of the corresponding phenoxyl radicals,[31-33] which have strong absorption bands around 390nm. The kinetic curve of decay of phenoxyl radical is easily differentiated from the quinoline **8d** species by the long lifetime decay generated in ethanol. Scheme 3 shows the electron transfer mechanism between quinoline **8d** (Q) and phenol (PhOH), where $PhOH^{\bullet}$ and $PhO^{\bullet}$ are the protonated and deprotonated phenol radicals. $Q(+H)^{\bullet+}$ is the semi-oxidized quinoline radical in protonated form.

$$^1Q_o \xrightarrow{h\nu} {}^1Q^* \xrightarrow{K_{ISC}} {}^3Q \xrightarrow{+Phenol} Q^{\bullet+}_{s-ox} + PhOH^{\bullet}$$

$$Q^{\bullet+}_{s-ox} + PhOH^{\bullet} \longrightarrow Q(+H)^{\bullet+} + PhO^{\bullet}$$

Scheme 3. Electron transfer mechanism between quinoline and phenol.

Following the electron transfer process in the triplet state of quinoline, the Rehm-Weller equation[34] can be written as:

$$\Delta G = E_{\left(\frac{D}{D+}\right)} - E_{\left(\frac{A}{A-}\right)} - E^* + \frac{Z_1 Z_2}{D r_{12}}$$

where E* is the energy of the triplet state (3.10 eV) and the last term is the coulombic energy necessary to form an ion pair with charges Z_1 and Z_2 in a medium of dielectric constant D at a distance r_{12}. The coulombic term can be neglected in a medium of high dielectric constant. $E_{(D/D+)}$ (+1.65 V from voltammetry) and $E_{(A/A-)}$ (+0.86 V *vs.* NHE)[35] are the potential, in volts, for the oxidation of quinoline and reduction of phenol, respectively. The negative free energy (ΔG_{et} = −242.20 kJ mol^{-1}) calculated by Rehm-Weller equation connects a favourable electron transfer

process between triplet-state of quinoline **8d** and phenol, indicating a good alternative for compounds that can be photo-activated, such as solar cells.

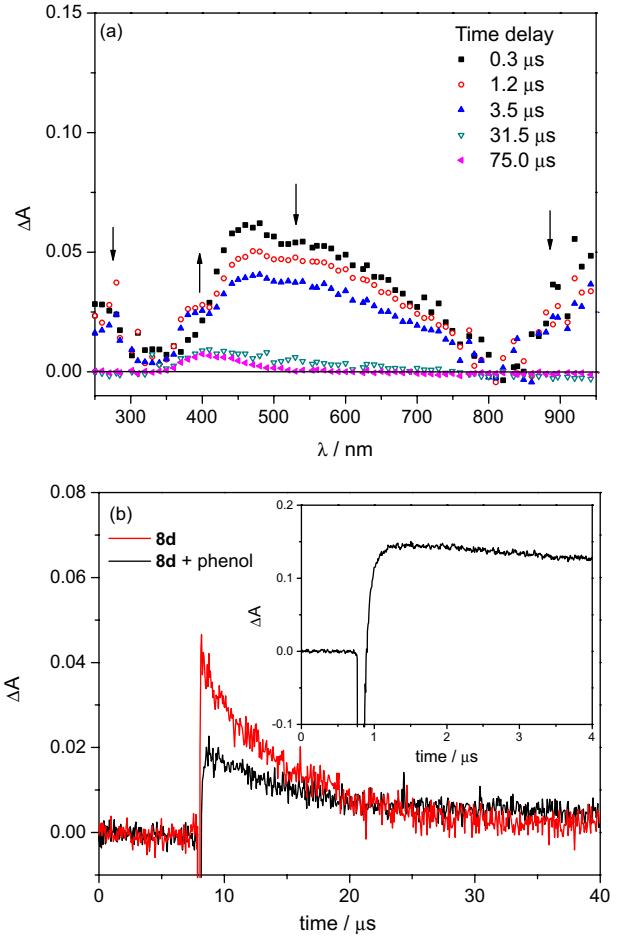

Figure 6. (a) Transient absorption spectrum for **8d** in the presence of phenol (1×10^{-4} mol L^{-1}) and (b) transient decay of **8d** in the presence and absence of phenol at 390 nm. Inset: growth and decay lifetime of **8d** + phenol solution monitored at 390 nm on a short timescale.

Conclusions

In summary, a three-component coupling reaction of aldehydes **2**, amines **4** and alkynes **7** mediated by Lewis acid $FeCl_3$ and $Yb(OTf)_3$ was applied to five new synthesised quinolines **8a**-**e**. **8a** is 4-aryl-8-alkyl disubstituted and **8b**-**e** is 2,4-diaryl-6-alkyl trisubstituted quinolines. The Yb^{3+} catalyst rendered the quinolines in better yields than Fe^{3+}. None of quinolines **8a**-**e** displayed LC behaviour, even the more anisotropic **8e**. The chemical structures of the quinolines were fully characterised by ^1H and ^{13}C nuclear magnetic resonance (NMR) and mass spectrometry (MS) analysis. **A** single-crystal X-ray analysis was also determined for **8e**. From a single-crystal structure, **8e** has a phenyl group and a pendant naphthyl group connected to the C2 and C4 carbon of the quinoline ring with torsion angles of 7.30° and 65.2°, respectively. The flexible alkyl located on the naphthyl group is randomly coiled. UV-Vis absorbance measurements of the quinolines in different dielectric constant media show two different bands at 280 and 350 nm, that were attributed to π,π* and n,π* transitions, respectively. In polar solvents, the quinoline **8d** presents a progressive red shift of the lowest-energy emission band at 400 nm and no change was observed to the lower-energy absorption band ($\varepsilon < 10^4$ mol^{-1} L cm^{-1}), which was characterised as n,π* transition. A laser flash photolysis study for **8d** connects a main transient band at 450 nm with a lifetime of 2.6 µs in ethanol that is totally quenched in the presence of oxygen. The transient was assigned to triplet-triplet absorption of quinoline **8d**, which is semi-oxidized in the presence of phenol by electron transfer.

Experimental

Spectral measurements

Absorption spectra, time-resolved fluorescence and electrochemistry data as well as crystallographic analysis are reported in the SI section.

Synthesis

All starting materials were purchased from commercial suppliers (Sigma Aldrich Chemical Co., Acros Organics and ABCR Chemicals) and used without further purification. All reactions were carried out under a nitrogen atmosphere in oven-dried glassware with magnetic stirring. Solvents were dried, purified and degassed under classical methods. Solvents used in extraction and purification were distilled prior to use. Thin layer chromatography (TLC) was performed using silica gel 60 F254 aluminum sheets and the visualization of the spots has been done under UV light (254 nm) or stained with iodine vapor. Products were purified by flash chromatography on silica gel 60 M, 230-400 mesh. Melting point was measured using an Olympus BX43 microscope equipped with a Mettler Toledo FP82HT Hot Stage FP90. ^1H (^{13}C) NMR spectra were recorded at 300 (75) MHz on a Varian Inova and 400 (100) MHz Bruker spectrometer using $CDCl_3$ as solvent. The ^1H and ^{13}C chemical shifts were reported in parts *per* million (δ) referenced to residual solvent signals at $\delta_{H/C}$ 7.26/77.00 ($CDCl_3$) relative to tetramethylsilane (TMS) as internal standard. Coupling constants *J* [Hz] were directly taken from the spectra and are not averaged. Splitting patterns are designated as s (singlet), d (doublet), t (triplet),

q (quartet), m (multiplet) and br (broad). Attenuated total reflection (ATR)/Fourier transform infrared (FTIR) spectra were recorded on a Varian FT-IR-640 spectrometer. Low-resolution mass spectra were obtained with a Shimadzu GC-MS-QP5050 mass spectrometer interfaced with a Shimadzu GC-17A gas chromatograph equipped with a DB-17 MS capillary column. High resolution mass spectrometry (HRMS) spectra were obtained from a Fourier transform ion cyclotron resonance (FT-ICR) mass spectrometer equipped with an Infinity™ cell, a 7.0 Tesla superconducting magnet, an RF-only hexapole ion guide and an external electrospray ion source (off axis spray) and with ESI(+)-MS and tandem ESI(+)-MS/MS using a hybrid high-resolution and high accuracy MicroTOF-Q II mass spectrometer (Bruker Daltonics), or on a Micromass Q-TOFmicro instrument.

General procedure for the synthesis of quinolines **8a-e**: A solution of aldehyde (1 mmol or 1.5 mmol for paraformaldehyde), aniline (1 mmol) and catalyst ($FeCl_3$ or $Yb(OTf)_3$ 10 mol%) in 5 mL of dry toluene was stirred for 10 min, subsequently, 1 equivalent of alkyne was added to this mixture. The solution was heated at azeotropic reflux under an air atmosphere until the reactants are consumed (ca. 48 h). When the procedure was realized using $Yb(OTf)_3$, the mixture was heated for 36 h at 80 °C. The dark reaction mixture was cooled and filtered through a celite plug covered with thin activated charcoal. After evaporation of the solvent, the crude product was purified by silica gel chromatography (95:5 hexane:CH_2Cl_2).

Data for 8-octyloxy-4-[4-(octyloxy)phenyl]quinoline (**8a**): Yield 12%; yellow solid; m.p. 68-70 °C; ^{1}H NMR (300 MHz, $CDCl_3$) δ 8.97 (d, *J* 4.3 Hz, 1H, Ar-H), 7.52 (dd, *J* 8.6 Hz, *J* 3.0 Hz, 1H, Ar-H), 7.45 (d, *J* 9.0 Hz, 2H, Ar-H), 7.41 (m, 1H, Ar-H), 7.34 (d, *J* 4.5 Hz, 1H, Ar-H), 7.08 (m, 1H, Ar-H), 7.05 (d, *J* 6.0 Hz, 2H, Ar-H), 4.28 (t, *J* 6.5 Hz, 2H, CH_2O), 4.06 (t, *J* 7 Hz, 2H, CH_2O), 2.07 (m, 2H, $C\underline{H}_2CH_2O$), 1.85 (m, 2H, $C\underline{H}_2CH_2O$), 1.58-1.38 (m, 24H, $(CH_2)_{12}$), 0.91 (m, 6H, $(CH_3)_2$); ^{13}C NMR (75 MHz, $CDCl_3$) δ 159.3, 155.0, 148.8, 148.1, 140.9, 130.8, 130.5, 128.2, 126.3, 121.8, 117.5, 114.5, 108.3, 69.1, 68.1, 31.9, 31.8, 29.6, 29.4 (2C), 29.3, 29.2 (2C), 29.1, 28.9, 26.1, 22.7, 22.6, 14.1.

Data for 6-methoxy-2-(4-methoxyphenyl)-4-[4-(octyloxy) phenyl]quinoline (**8b**): Yield 40%; yellow solid; m.p. 85-86 °C; ^{1}H NMR (300 MHz, $CDCl_3$) δ 8.11 (m, 3H), 7.70 (s, 1H), 7.49 (d, *J* 8.8 Hz, 2H, Ar-H), 7.36 (dd, *J* 9.2 Hz, *J* 2.8 Hz, 1H, Ar-H), 7.22 (d, *J* 2.6 Hz, 1H, Ar-H), 7.05 (m, 4H, Ar-H), 4.05 (t, *J* 7 Hz, 2H, CH_2O), 3.87 (s, 3H, OCH_3), 3.80 (s, 3H, OCH_3), 1.85 (m, 2H, $C\underline{H}_2CH_2O$), 1.55-1.25 (m, 10H, $(CH_2)_5$), 0.90 (t, 3H, CH_3); ^{13}C NMR (75 MHz, $CDCl_3$) δ 160.6, 159.5, 157.6, 154.5, 147.7, 145.0, 132.6, 131.5, 131.0, 130.7, 128.7, 126.7, 121.8, 119.4, 114.8, 114.3, 103.9, 68.4, 55.6, 55.5, 32.0, 29.6, 29.5, 29.4, 26.3, 22.9, 14.3; HRMS (ESI) *m/z* $[M + H]^+$ calcd. for $C_{31}H_{36}NO_3^+$: 470.2690; found: 470.2695.

Data for 4-(4-heptyloxyphenyl)-6-methoxy-2-[4-(octyloxy)phenyl]quinoline (**8c**): Yield 13% (10 mol% $FeCl_3$) and 60% (10 mol% $Yb(OTf)_3$); yellow solid; m.p. 75-76 °C; ^{1}H NMR (300 MHz, $CDCl_3$) δ 8.10 (m, 3H, Ar-H), 7.70 (s, 1H, Ar-H), 7.49 (d, *J* 6.0 Hz, 2H, Ar-H), 7.36 (dd, *J* 9.0 Hz, *J* 2.9 Hz, 1H, Ar-H), 7.21 (d, *J* 2.8 Hz, 1H, Ar-H), 7.06 (d, *J* 6.0 Hz, 2H, Ar-H), 7.02 (d, *J* 9.0 Hz, 2H, Ar-H), 4.04 (m, 4H, $(CH_2O)_2$), 3.80 (s, 3H, OCH_3), 1.83 (m, 4H, $(C\underline{H}_2CH_2O)_2$), 1.53-1.30 (m, 18H), 0.90 (m, 6H, $(CH_3)_2$); ^{13}C NMR (75 MHz, $CDCl_3$) δ 160.1, 159.3, 157.4, 154.4, 147.4, 144.9, 132.2, 131.3, 130.9, 130.6, 128.5, 126.5, 121.6, 119.7, 114.7, 114.6, 103.8, 68.2, 68.1, 55.4, 31.9, 31.8, 29.5, 29.4, 29.3, 29.2, 26.1, 22.7 (2C), 14.2.

Data for 4-[(6-heptyloxynaphthalen)-2-yl]-6-methoxy-2-[4-(octyloxy)phenyl] quinoline (**8d**): Yield 40%; yellow solid; m.p. 87-88 °C; ^{1}H NMR (300 MHz, $CDCl_3$) δ 8.13 (m, 3H, Ar-H), 7.96 (d, *J* 1.3 Hz, 1H, Ar-H), 7.88 (d, *J* 8.4 Hz, 1H, Ar-H), 7.81 (m, 2H, Ar-H), 7.64 (dd, *J* 8.4 Hz, 1.8 Hz, 1H, Ar-H), 7.38 (dd, *J* 9.2 Hz, 2.9 Hz, 1H, Ar-H), 7.23 (m, 3H, Ar-H), 7.02 (d, 2H, *J* 8.4 Hz, Ar-H), 4.13 (t, 2H, CH_2O), 4.03 (t, *J* 6.8 Hz, 2H, CH_2O), 3.75 (s, 3H, OCH_3), 1.89 (m, 2H, $C\underline{H}_2CH_2O$), 1.82 (m, 2H, $C\underline{H}_2CH_2O$), 1.55-1.34 (m, 18H, $(CH_2)_9$); 0.91 (m, 6H, $(CH_3)_2$); ^{13}C NMR (75 MHz, $CDCl_3$) δ 160.1, 157.8, 157.5, 154.4, 147.8, 144.9, 134.3, 133.9, 132.2, 131.4, 129.6, 128.8, 128.5, 128.3, 127.7, 127.0, 126.9, 126.6, 121.7, 119.8, 119.4, 114.8, 106.5, 103.8, 68.2, 68.1, 55.4, 31.8, 29.4, 29.3, 29,2, 29.1, 26.1, 26.0, 22.7, 22.6, 14.1; HRMS (ESI) *m/z* $[M + H]^+$ calcd. for $C_{41}H_{50}NO_3^+$: 604.3785; found: 604.3793.

Data for 4-[(6-heptyloxynaphthalen)-2-yl]-6-nonyloxy-2-[4-(octyloxyphenyl] quinoline (**8e**): Yield 36%; yellow solid; m.p. 67-68 °C; ^{1}H NMR (300 MHz, $CDCl_3$) δ 8.39 (m, 1H, Ar-H), 8.18 (d, *J* 8.2 Hz, 2H, Ar-H), 7.97 (s, 1H, Ar-H), 7.91-7.82 (m, 3H, Ar-H), 7.63 (dd, *J* 8.2 Hz, *J* 1.8 Hz, 1H, Ar-H), 7.42 (dd, *J* 9.4 Hz, 2.3 Hz, 1H, Ar-H), 7.27-7.22 (m, 3H, Ar-H), 7.05 (d, *J* 8.8 Hz, 2H, Ar-H), 4.14 (t, *J* 6.5 Hz, 2H, CH_2O), 4.04 (t, *J* 6.5 Hz, 2H, CH_2O), 3.89 (t, *J* 6.5 Hz, 2H, CH_2O), 1.94-1.70 (m, 6H, $(C\underline{H}_2CH_2O)_3$), 1.60-1.22 (m, 30H, $(CH_2)_{15}$), 0.89 (m, 9H, $(CH_3)_3$); ^{13}C NMR (75 MHz, $CDCl_3$) δ 160.1, 157.8, 157.0, 154.2, 147.7, 144.8, 134.3, 134.0, 132.2, 131.2, 129.6, 128.8, 128.5, 128.2, 127.7,

126.9, 126.5, 121.9, 119.8, 119.4, 114.7, 106.4, 104.6, 68.2, 68.1, 55.4, 31.9, 31.8, 29.5, 29.4, 29.3, 29.2, 29.1 (2C), 26.1, 26.0 (2C), 22.4, 14.1; HRMS (ESI) *m/z* $[M + H]^+$ calcd. for $C_{49}H_{66}NO_3^+$: 716.6037; found: 716.5043.

Supplementary Information

Supplementary data are available free of charge at http://jbcs.sbq.org.br as PDF file.

Acknowledgments

The authors gratefully acknowledge INCT-Catálise, edital 01/12-PPG-Química-UFRGS, Fapergs-edital PqG 2012, FINEP and FAPESP 12/19823-4 for financial support. Thanks to LDRX-DF/UFSC for X-ray diffraction experiments. The authors are also grateful to Sidnei Moura e Silva (Universidade de Caxias do Sul) for the HRMS analysis. Eric S. Sales thanks PIBIC-UFRGS for his fellowship.

References

1. Friedlander, P.; *Ber. Dtsch. Chem. Ges.* **1882**, *15*, 2572.
2. da Costa, J. S.; Pisoni, D. S.; Silva, C. B.; Petzhold, C.; Russowsky, D.; Ceschi, M. A.; *J. Braz. Chem. Soc.* **2009**, *20*, 1448.
3. Nosten, F.; McGready, R.; d'Alessandro, U.; Bonell, A.; Verhoeff, F.; Menendez, C.; Mutabingwa, T.; Brabin, B.; *Curr. Drug Saf.* **2006**, *1,* 1.
4. Parke, A.; *Am. J. Med.* **1988**, *85*, 30.
5. Roepe, P. D.; *Trends Parasitol.* **2014**, *30*, 130.
6. Baird, J. K.; Hoffman, S. L.; *Clin. Infect. Dis.* **2004**, *39*, 1336.
7. Santos, M. S.; Del Lama, M. P. F. M.; Ito, A. S.; Naal, R. M. Z. G.; *J. Lumin.* **2014**, *147*, 49.
8. Cinar, R.; Nordmann, J.; Dirksen, E.; Müller, T. J. J.; *Org. Biomol. Chem*. **2013**, *11*, 2597.
9. Staderini, M.; Aulić, S.; Bartolini, M.; Tran, H. N. A.; González-Ruiz, V.; Pérez, D. I.; Cabezas, N.; Martínez, A.; Martín, A. M.; Andrisano, V.; Legname, G.; Menéndez, J. C.; Bolognesi, M. L.; *ACS Med. Chem. Lett.* **2013**, *4*, 225.
10. Ueno, T.; Nagano, T.; *Nat. Methods* **2011**, *8*, 642.
11. Kappaun, S.; Slugove, C.; List, E. J. W.; *Int. J. Mol. Sci.* **2008**, *9*, 1527; Park, J.; Park, J. S.; Park, Y. G.; Lee, J. Y.; Kang, J. W.; Liu, J.; Daí, L.; Jin, S.-H.; *Org. Electron.* **2013**, *14*, 2114; Li, J.; Wang, R.; Yang, R.; Zhou, W.; Wang, X.; *J. Mater. Chem. C* **2013**, *1*, 4171; Tonzola, C. J.; Alam, M. M.; Kaminsky, W.; Jenekhe, S. A.; *J. Am. Chem. Soc.* **2003**, *125*, 13548.
12. Cao, K.; Zhang, F-M.; Tu, Y-Q.; Zhuo, X-T.; Fan, C-A.; *Chem. Eur. J.* **2009**, *15*, 6332; Russowsky, D.; Benvenutti, E. V.; Roxo, G. S.; Graesel, F.; *Lett. Org. Chem.* **2007**, *4*, 97.
13. Elangovan, A.; Chen, T-Y.; Chen, C-Y.; Ho, T-I.; *Chem. Commun*. **2003**, 2146; Elangovan, A.; Yang, S-W.; Lin, J-H.; Kao, K-M.; Ho, T-I.; *Org. Biomol. Chem*. **2004**, *2*, 1597; Si, G.; Zhao, Y.; Leong, E. S. P.; Liu, Y. J.; *Materials* **2014**, *7*, 1296; Gamba, M-G.; Yu, C. H.; Tang, B. J.; Welch, C.; Kohlmeier, A.; Schubert, C. P.; Mehl, G. H.; *Materials* **2014**, *7*, 3494.
14. Tavares, A.; Livotto, P. R.; Gonçalves, P. F. B.; Merlo, A. A.; *J. Braz. Chem. Soc.* **2009**, *20*, 1742; Vasconcelos, U. B.; Schrader, A.; Vilela, G. D.; Borges, A. C. A.; Merlo, A. A.; *Tetrahedron* **2008**, *64,* 4619.
15. Merlo, A. A.; Livotto, P. R.; Gallardo, H. A. O.; Taylor, T. R.; *Mol. Cryst. Liq. Cryst.* **1998**, *309*, 111.
16. Vogel, A. I.; *Vogel´s Textbook of Practical Organic Chemistry,* 5th ed.; England Longman Scientific & Technical, 1991; Markiewicz, J. T.; Wiest, O.; Helquist, P.; *J. Org. Chem*. **2010**, *75*, 4887.
17. Vasconcelos, U. B.; Dalmolin, E.; Merlo, A. A.; *Org. Lett*. **2005**, *7*, 1027; Vasconcelos, U. B.; Merlo, A. A.; *Synthesis* **2006**, 1141.
18. Bolm, C.; Legros, J.; Paih, J. L.; Zani, L.; *Chem. Rev*. **2004**, *104*, 6217; Correa, A.; Mancheño, O. G.; Bolm, C.; *Chem. Soc. Rev*. **2008**, *37*, 1108; Enthaler, S.; Junge, K.; Beller, M.; *Angew. Chem., Int. Ed.* **2008**, *47*, 3317; Sherry, B. D.; Fürstner, A.; *Acc. Chem. Res*. **2008**, *4*, 1500.
19. Sueki, S.; Okamoto, C.; Shimizu, I.; Seto, K.; Furukawa, Y.; *Bull. Chem. Soc. Jpn*. **2010**, *83*, 385.
20. Tang, J.; Wang, L.; Mao, D.; Wang, W.; Zhang, L.; Wu, S.; Yongshu-Xie, Y.; *Tetrahedron* **2011**, *67*, 8465.
21. Cao, K.; Zhang, F.-M.; Tu, Y.-Q.; Zhuo, X.-T.; Chun-An Fan, C.-A.; *Chem. Eur. J*. **2009**, *15*, 6332.
22. Xiao, F.; Chen, Y.; Liu, Y.; Wang, J.; *Tetrahedron* **2008**, *64*, 2755.
23. Albaladejo, M. J.; Alonso, F.; Moglie, Y.; Yus, M.; *Eur. J. Org. Chem.* **2012**, *2012*, 3093.
24. Mamane, V.; Hannen, P.; Furstner, A.; *Chem. Eur. J.* **2004**, *10*, 4556.
25. Liu, P.; Wang, Z.; Lin, J.; Hu, X.; *Eur. J. Org. Chem*. **2012**, *2012*, 1583.
26. Souza, B. S.; Nome, F.; *J. Org. Chem*. **2010**, *75*, 7186.
27. Pavia, D. L.; Lampman, G. M.; Kriz, G. S.; *Introduction to Spectroscopy. A Guide for Students of Organic Chemistry*, 2nd ed.; Saunders College Publishing, 1996.
28. Vincent, J. S.; Maki, A. H.; *J. Chem. Phys.* **1965**, *42*, 865; Ramasamy, S. M.; Hurtubise, R. J.; *Anal. Chim. Acta* **1983**, *152*, 83; Jones, G.; *The Chemistry of Heterocyclic Compounds, Quinolines,* John Wiley & Sons: London, 1977.
29. Zhenming, D.; Heping, S.; Yufang, L.; Diansheng, L.; Bo, L.; *Spectrochim. Acta, Part A* **2011**, *78*, 1143; Chaia, S.; Conga, S-L.; *Comput. Theor. Chem.* **2014**, *1034*, 80; Sutariya, P. G.; Modi, N. R.; Pandya, A.; Joshi, B. K.; Joshia, K. V.; Menon, S. K.; *Analyst* **2012**, *137*, 5491; Aleksandrova, E. L.; Svetlichnyi, V. M.; Myagkova, L. A.; Matyushina, N. V.; Nekrasova,

T. N.; Smyslov, R. Y.; Pautov, V. D.; Tameev, A. R.; Vannikov, A. V.; Kudryavtsev, V. V.; *Opt. Spectrosc.* **2013**, *114*, 737; Zhenming, D.; Heping, S.; Yufang, L.; Diansheng, L.; Bo, L.; *Spectrochim. Acta, Part A* **2011**, *78*, 1143.

30. Nedoloujko, A.; Kiwi, J.; *J. Photochem. Photobiol., A* **1997**, *110*, 141; Tanimoto, Y.; Takase, S.; Jinda, C.; Kyotani, M.; Itoh, M.; *Chem. Phys.* **1992**, *162*, 7.
31. Biczók, L.; Bérces, T.; Linschitz, H.; *J. Am. Chem. Soc*. **1997**, *119*, 11071.
32. Das, P. K.; Encinas, M. V.; Scaiano, J. C.; *J. Am. Chem. Soc*. **1981**, *103*, 4154.
33. Miranda, M. A.; Lahoz, A.; Boscá, F.; Metni, M. R.; Abdelouahoa, F. B.; Castell, J. V.; Peréz-Prieto, J.; *Chem. Commun*. **2000**, 2257; Miranda, M. A.; Lahoz, A.; Martínez-Mánez, R.; Boscá, F.; Castell, J. V.; Perez-Prieto, J.; *J. Am. Chem. Soc.* **1999**, *121*, 11569.
34. Rosspeintner, A.; Kattnig, D. R.; Angulo, G.; Landgraf, S.; Grampp, G.; *Chem. Eur. J.* **2008**, *14*, 6213; Neumann, M. G.; Pastre, I. A.; Previtali, C. M.; *J. Photochem. Photobiol., A* **1991**, *61*, 91.
35. Li, C.; Hoffman, M. Z.; *J. Phys. Chem. B* **1999**, *103*, 6653; Harriman, A.; *J. Phys. Chem*. **1987**, *91*, 6102.

Submitted: September 10, 2014
Published online: January 30, 2015

FAPERGS and FAPESP have sponsored the publication of this article.

J. Braz. Chem. Soc., Vol. 26, No. 3, S1-S14, 2015.
Printed in Brazil - ©2015 Sociedade Brasileira de Química
0103 - 5053 $6.00+0.00

Supplementary Information

Quinolines by Three-Component Reaction: Synthesis and Photophysical Studies

Eric S. Sales,[a] Juliana M. F. M. Schneider,[a] Marcos J. L. Santos,[a] Adailton J. Bortoluzzi,[b] Daniel R. Cardoso,[c] Willy G. Santos*,[c] and Aloir A. Merlo*,[a]

[a]Instituto de Química, Universidade Federal do Rio Grande do Sul (UFRGS), 90040-060 Porto Alegre-RS, Brazil

[b]Departamento de Química, Universidade Federal de Santa Catarina(UFSC), 88040-900 Florianópolis-SC, Brazil

[c]Chemistry Institute of São Carlos, Universidade de São Paulo (USP), 13566-590 São Carlos-SP, Brazil

Experimental data

Data for 4-*n*-octyloxybenzaldehyde (**2a**). ^{1}H NMR (300 MHz, $CDCl_3$) δ (ppm) 9.87 (s, 1H, CHO), 7.83 (d, *J* 8.4 Hz, 2H, Ar-H), 6.99 (d, *J* 8.4 Hz, 2H, Ar-H), 4.05 (t, *J* 7.0 Hz, 2H, CH_2O), 1.78 (m, 2H, $C\underline{H}_2CH_2O$), 1.53-1.22 (m, 10H, $(CH_2)_5$), 0.89 (t, *J* 7.0 Hz, 3H, CH_3).

Data for 4-*n*-nonyloxyaniline (**4a**). Yield 90%; white solid; m.p. 42 °C; ^{1}H NMR (300 MHz, $CDCl_3$) δ (ppm) 7.17 (d, *J* 8.5 Hz, 2H, Ar-H), 6.80 (d, *J* 8.8 Hz, 2H, Ar-H), 6.08 (broad, 2H, NH_2), 3.89 (t, *J* 6.5 Hz, 2H, CH_2O), 1.77 (m, 2H, $C\underline{H}_2CH_2O$), 1.45-1.39 (m, 12H, $(CH_2)_6$), 0.89 (t, *J* 7.0 Hz, 3H, CH_3).

Data for 2-*n*-octyloxyaniline (**4b**). Yield 93%; white wax; ^{1}H NMR (300 MHz, $CDCl_3$) δ (ppm) 6.83 (m, 4H, Ar-H), 4.26 (broad, 2H, NH_2), 4.01 (t, *J* 6.8 Hz, 2H, CH_2O), 1.85 (m, 2H, $C\underline{H}_2CH_2O$), 1.54-1.38 (m, 10H, $(CH_2)_5$), 0.90 (q, *J* 7 Hz, 3H, CH_3).

4-methoxyaniline (*p*-anisidine) (**4c**) was purchased from Aldrich Co.

Data for 1-ethynyl-4-heptyloxybenzene (**7a**). Yield 70%; colorless oil; ^{1}H NMR (300MHz, $CDCl_3$) δ (ppm) 7.26 (d, *J* 8.5 Hz, 2H, Ar-H), 6.67 (d, *J* 8.4 Hz, 2H, Ar-H), 3.77 (t, *J* 6.0 Hz, 2H, CH_2O), 2.85 (s, 1H, CCH), 1.63 (m, 2H, $C\underline{H}_2CH_2O$), 1.30-1.20 (m, 8H, $(CH_2)_4$), 0.78 (t, *J* 6.5 Hz, 3H, CH_3); ^{13}C NMR (75 MHz, $CDCl_3$) δ (ppm) 160.13, 134.09, 115.00, 114,59, 84.36, 76.30, 68.58, 32.42, 29.83, 29.71, 26.61, 23.25, 14.69.

Data for 1-ethynyl-4-octyloxybenzene (**7b**). Yield 85%; colorless oil; ^{1}H NMR (300 MHz, $CDCl_3$) δ (ppm) 7.45 (d, *J* 8.5 Hz, 2H, Ar-H), 6.85 (d, *J* 8.4 Hz, 2H, Ar-H), 3.94 (t, *J* 6.0 Hz, 2H, CH_2O), 3.02 (s, 1H, CCH), 1.80 (m, 2H, $C\underline{H}_2CH_2O$), 1.50-1.32 (m, 8H, $(CH_2)_4$), 0.94 (t, *J* 6.5 Hz, 3H, CH_3); ^{13}C NMR (75 MHz, $CDCl_3$) δ (ppm) 159.53, 133.56, 133.53, 114.41, 113.96, 83.78, 75.72, 68.00, 31.89, 29.43, 29.32, 29.23, 26.08, 22.73, 14.15.

Data for 2-ethynyl-6-heptyloxynaphthalene (**7c**). Yield 83%; white solid; ^{1}H NMR (300 MHz, $CDCl_3$) δ (ppm) 7.94 (s, 1H, Ar-H), 7.67 (m, 2H, Ar-H), 7.47 (m, 1H, Ar-H), 7.15 (dd, *J* 9.0 Hz, *J* 2.5 Hz, 1H, Ar-H), 7.05 (d, *J* 2.6 Hz, 1H, Ar-H), 4.05 (t, *J* 7.0 Hz, 2H, CH_2O), 3.10 (s, 1H, CCH), 1.84 (m, 2H, $C\underline{H}_2CH_2O$), 1.50-1.30 (m, 8H, $(CH_2)_4$), 0.89 (t, *J* 6.5 Hz, 3H, CH_3); ^{13}C NMR (75 MHz, $CDCl_3$) δ (ppm) 158.02, 134.48, 132.10, 129.25, 129.08, 128.21, 126.81, 119.83, 116.80, 106.47, 84.33, 76.73, 76.68, 68.08, 31.86, 29.25, 29.16, 26.11, 22.70, 14.18.

*e-mail: aloir.merlo@ufrgs.br, willy_glen@yahoo.com.br

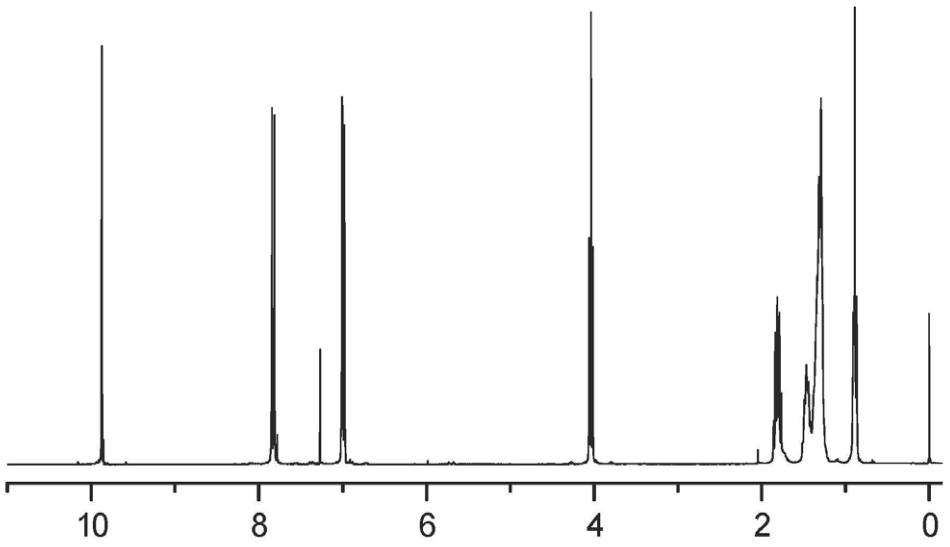

Figure S1. ^{1}H NMR (300 MHz, $CDCl_3$) spectrum of compound **2a**.

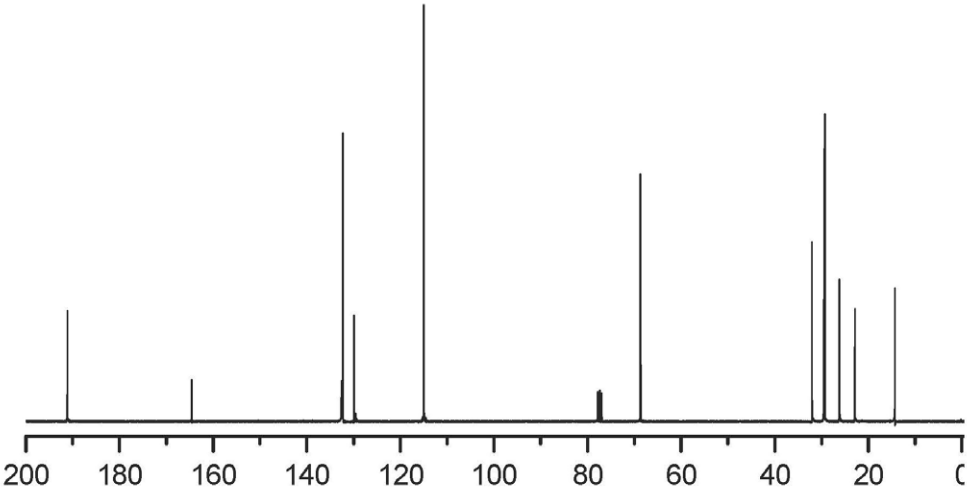

Figure S2. ^{13}C NMR (75 MHz, $CDCl_3$) spectrum of compound **2a**.

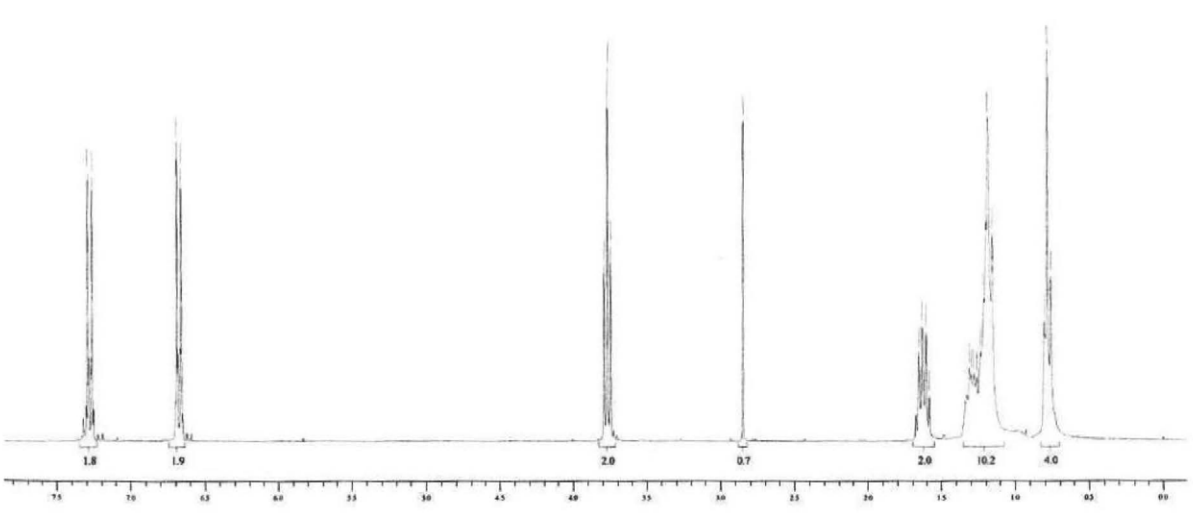

Figure S3. ^{1}H NMR (300 MHz, $CDCl_3$) spectra of **7a**.

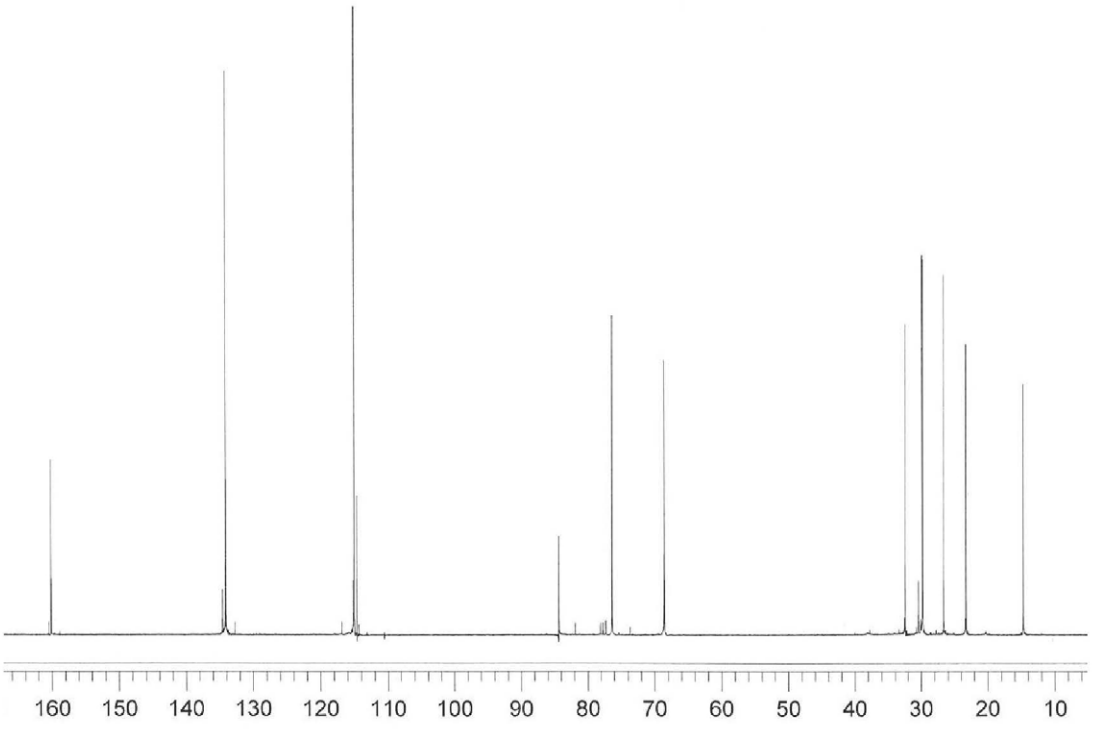

Figure S4. ^{13}C NMR (75 MHz, $CDCl_3$) spectra of **7a**.

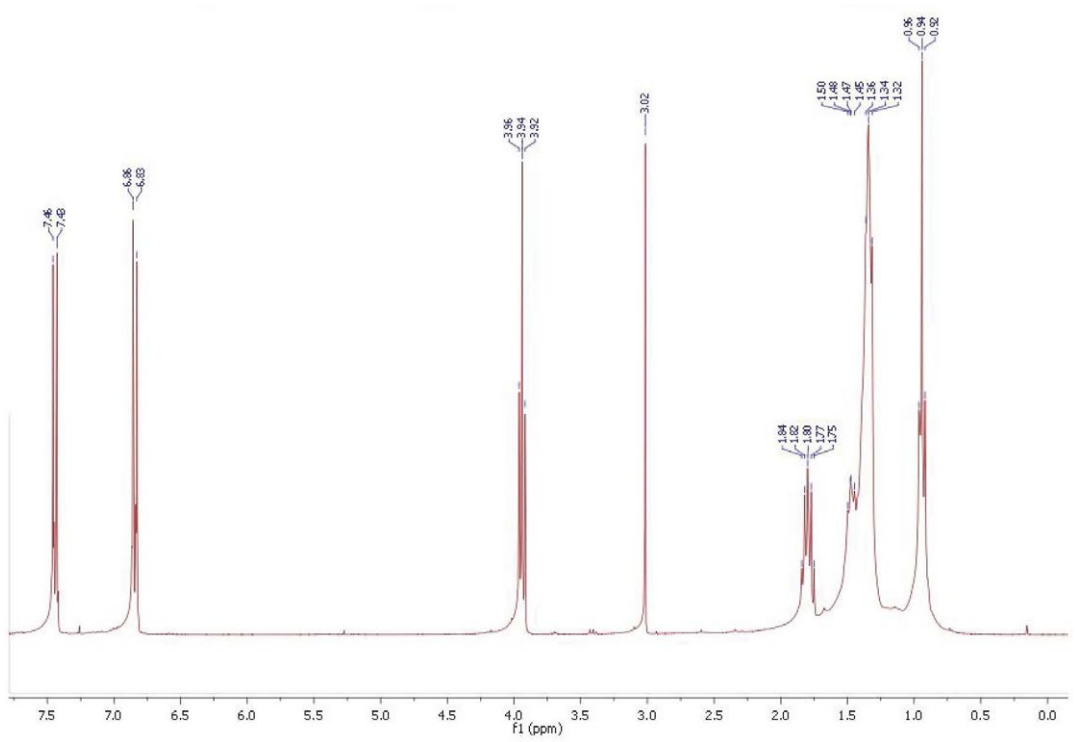

Figure S5. ^{1}H NMR (300 MHz, $CDCl_3$) spectra of **7b**.

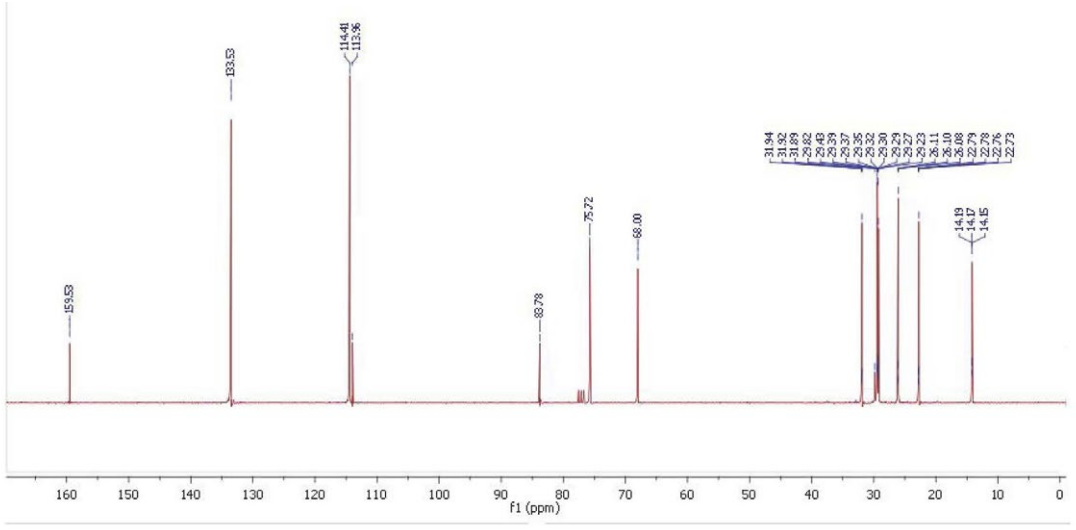

Figure S6. ^{13}C NMR (75 MHz, $CDCl_3$) spectra of **7b**.

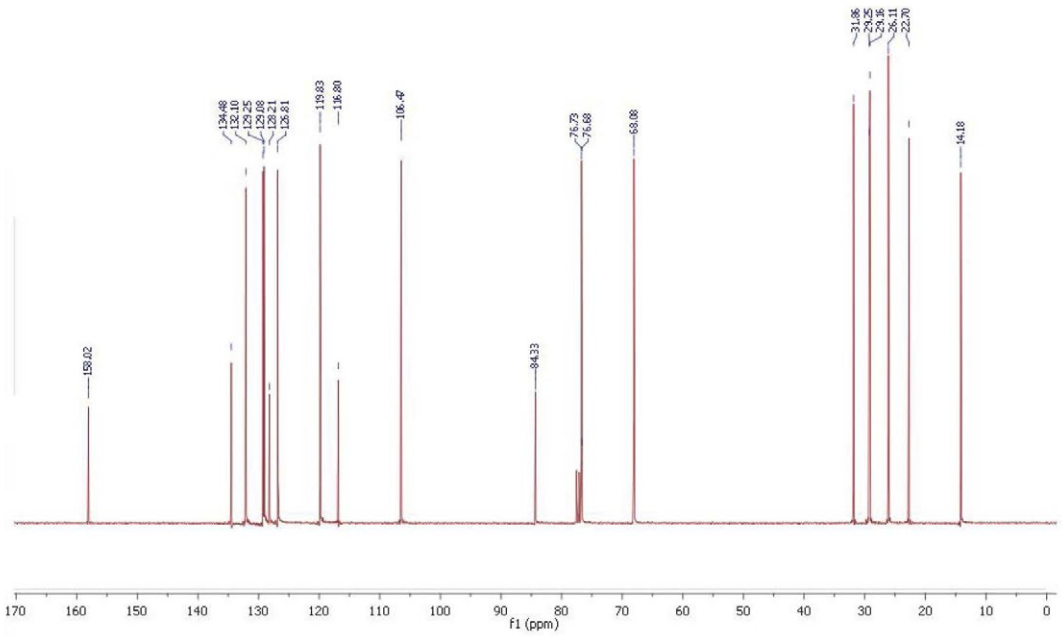

Figure S7. ^{13}C NMR (75 MHz, $CDCl_3$) spectra of **7c**.

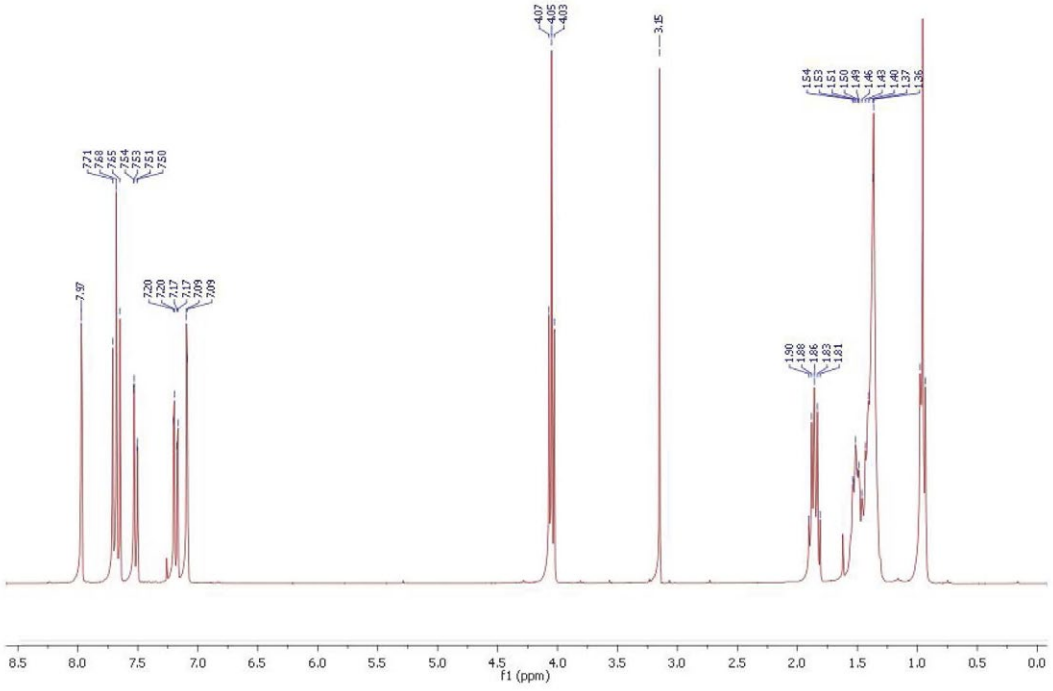

Figure S8. ^{1}H NMR (300 MHz, $CDCl_3$) spectra of **7c**.

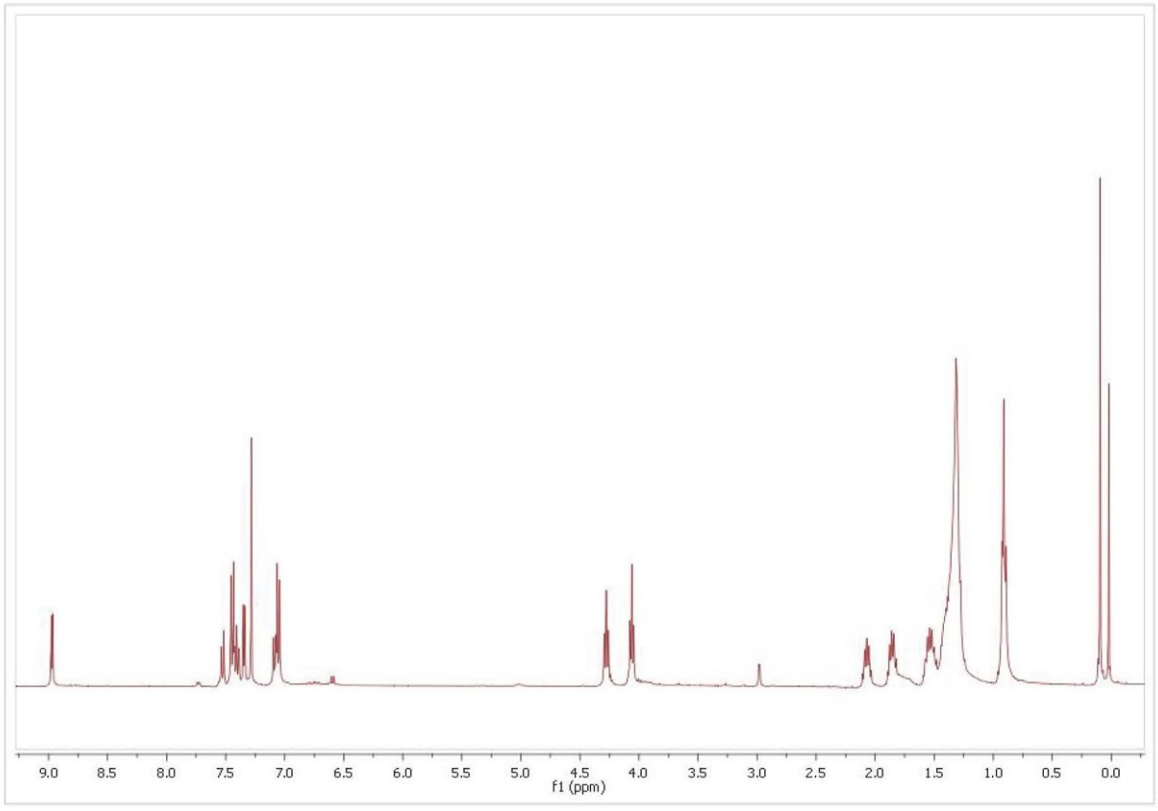

Figure S9. ^{1}H NMR (300 MHz, $CDCl_3$) spectra of compound **8a**.

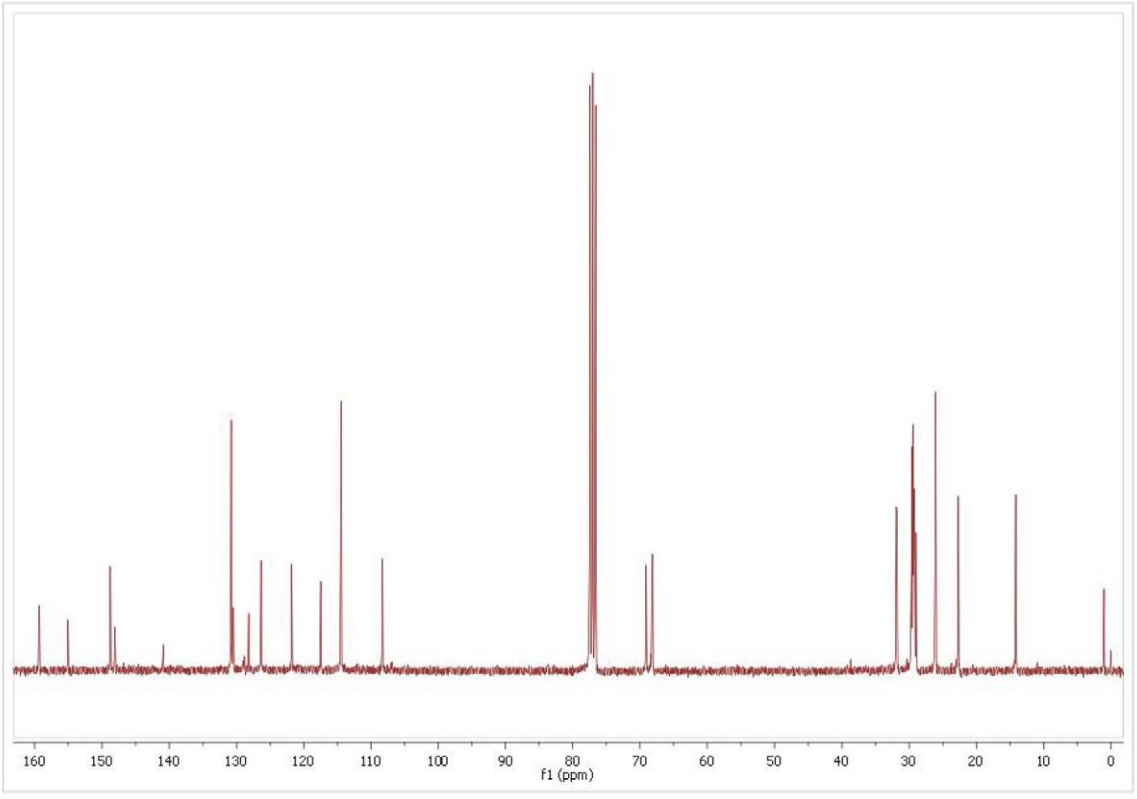

Figure S10. ^{13}C NMR (75 MHz, $CDCl_3$) spectra of compound **8a**.

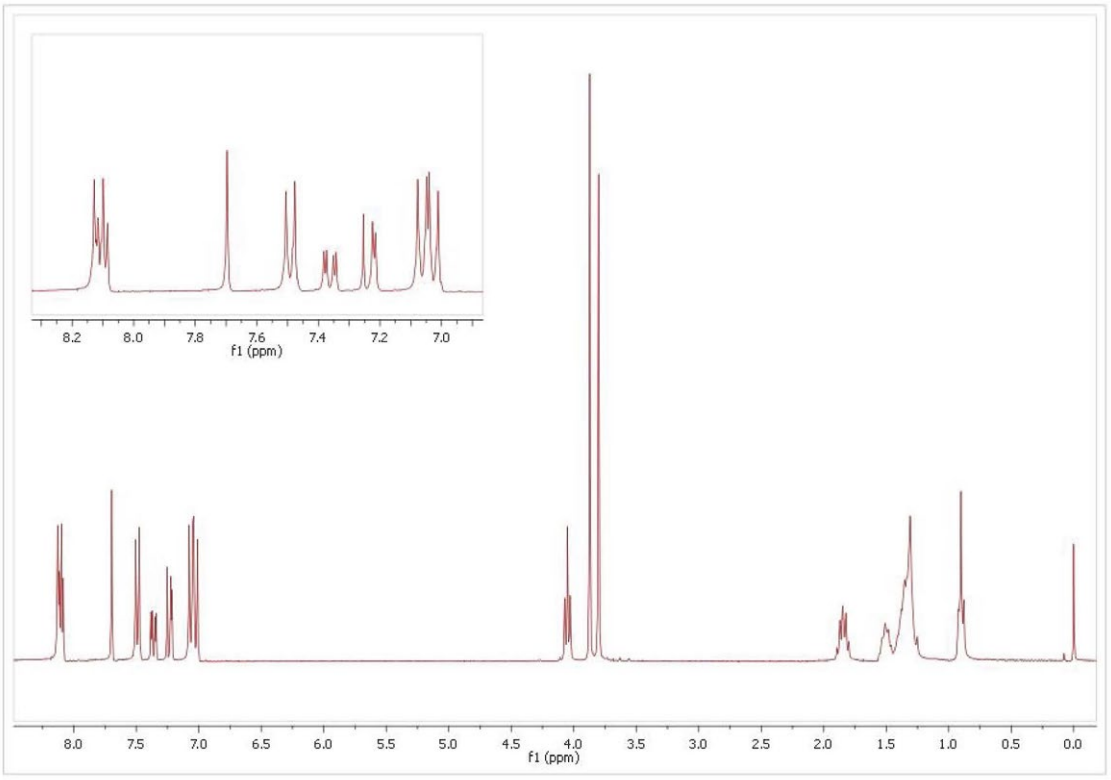

Figure S11. ^{1}H NMR (300 MHz, $CDCl_3$) spectra of compound **8b**.

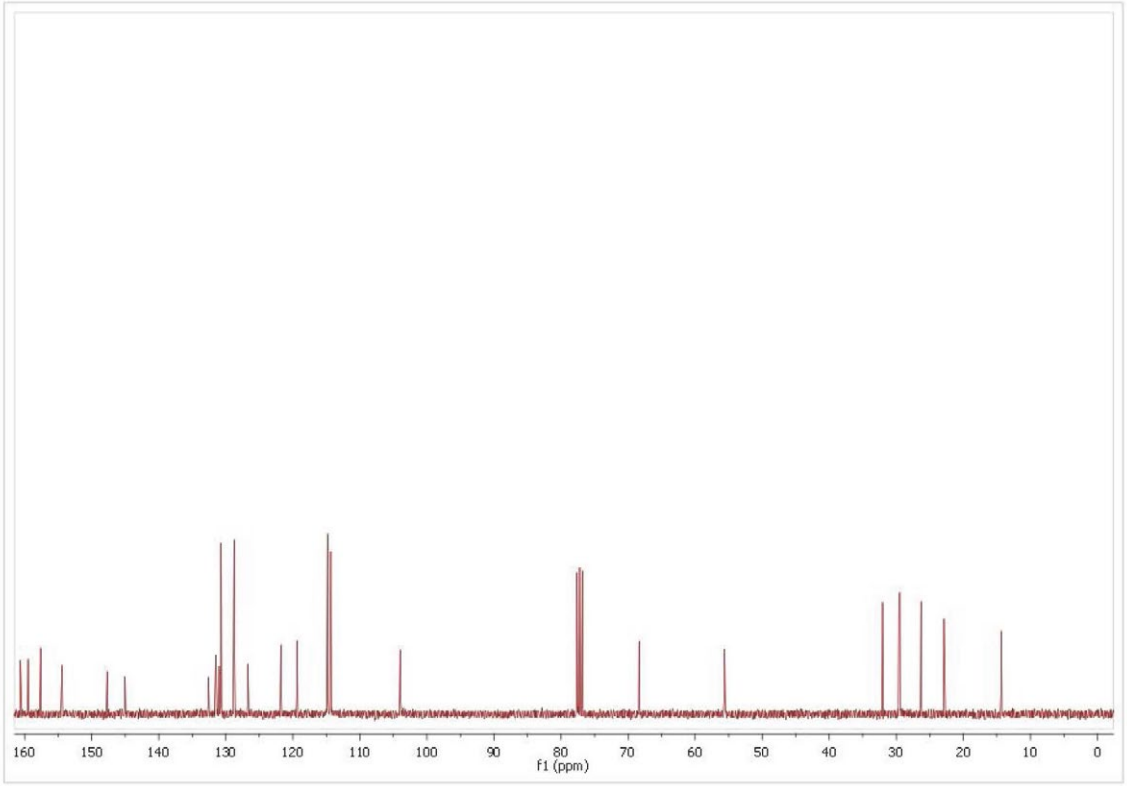

Figure S12. ^{13}C NMR (75 MHz, $CDCl_3$) spectra of compound **8b**.

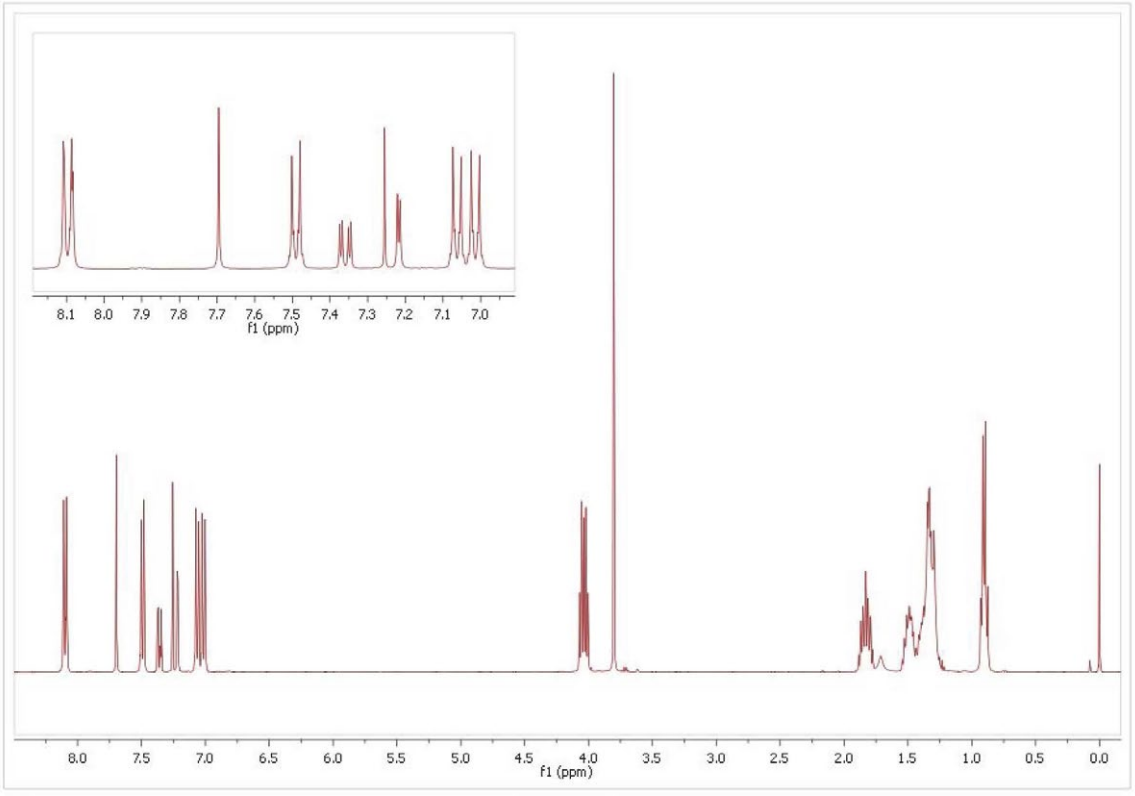

Figure S13. ^{1}H NMR (300 MHz, $CDCl_3$) spectra of compound **8c**.

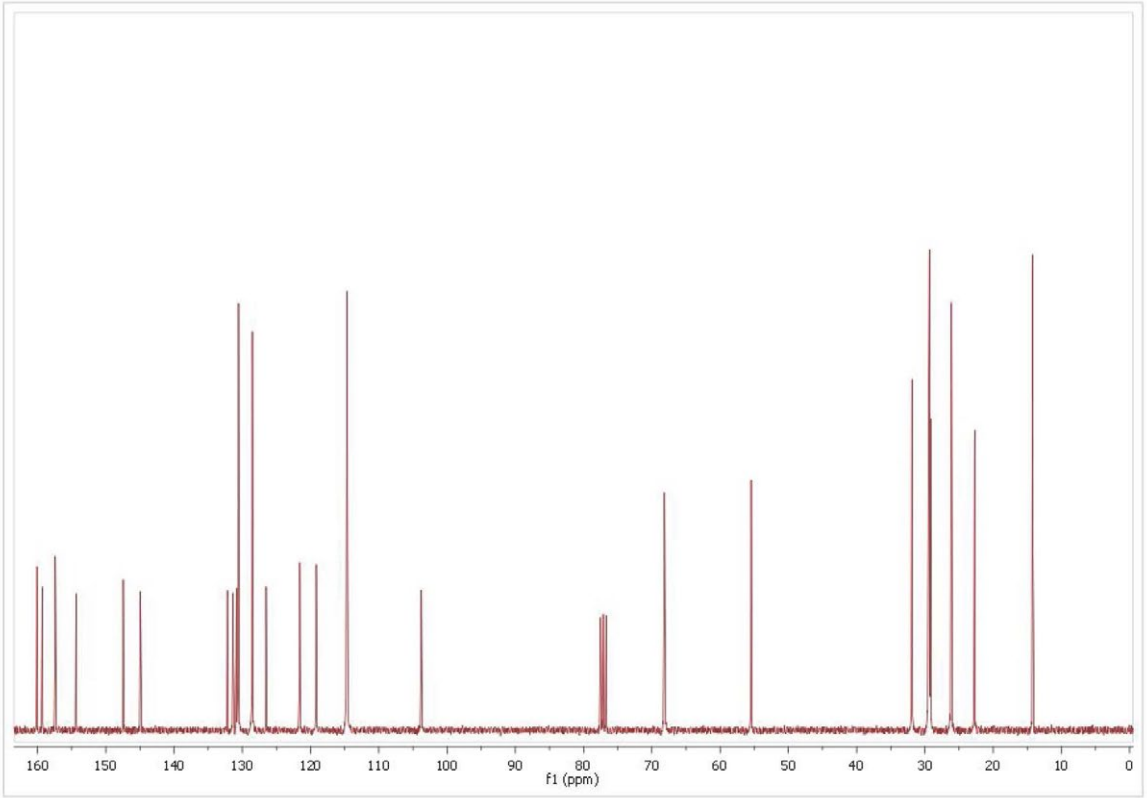

Figure S14. ^{13}C NMR (75 MHz, $CDCl_3$) spectra of compound **8c**.

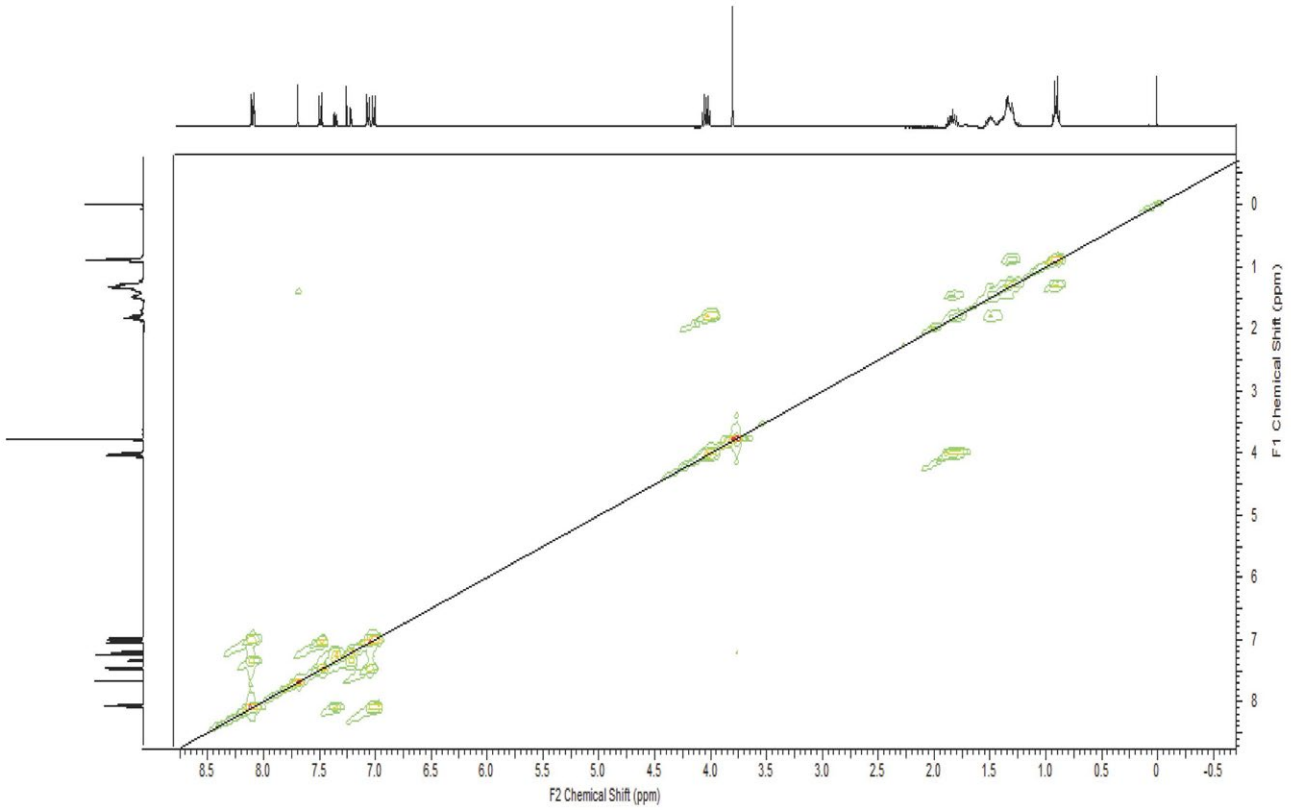

Figure S15. COSY ($CDCl_3$) spectra of compound **8c**.

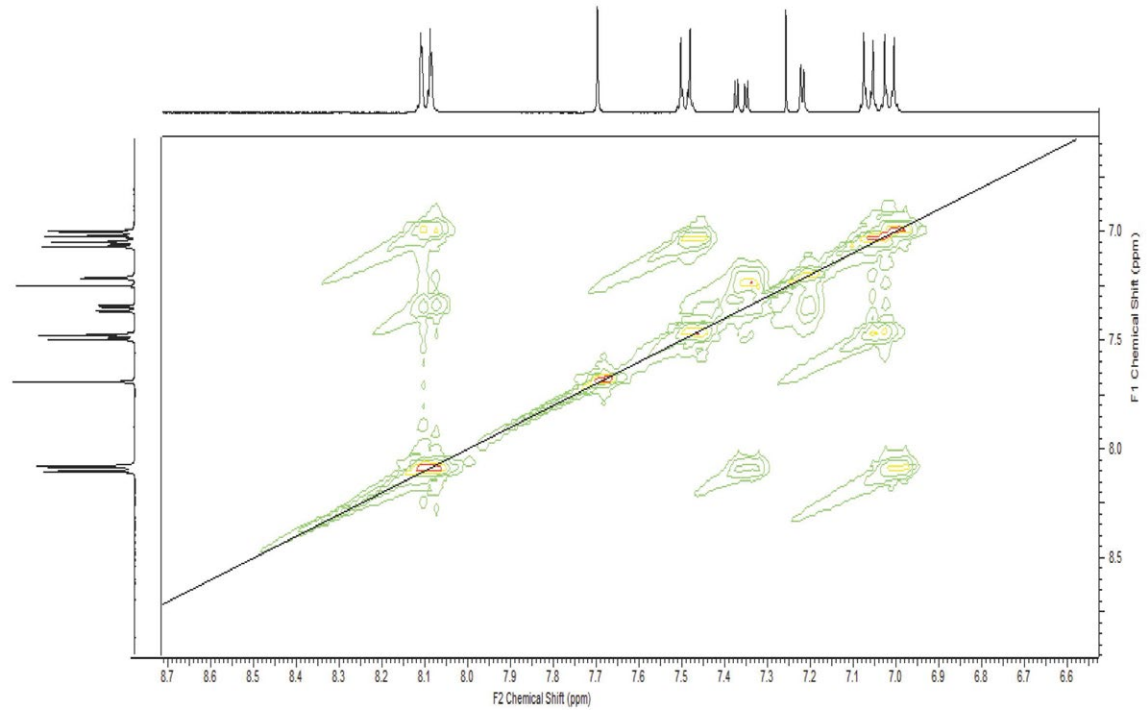

Figure S16. COSY ($CDCl_3$) spectra of compound **8c**. Aromatic region expansion.

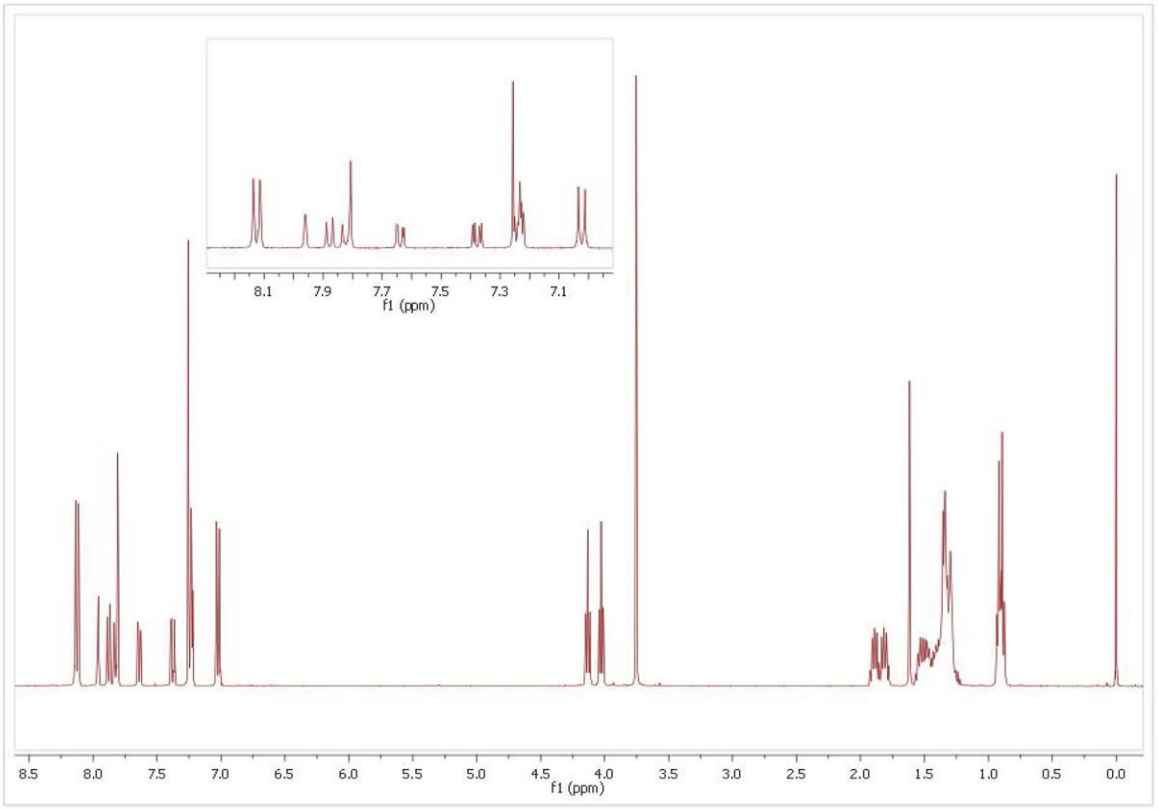

Figure S17. ^{1}H NMR (300 MHz, $CDCl_3$) spectra of compound **8d** (1.62ppm-H_2O peak).

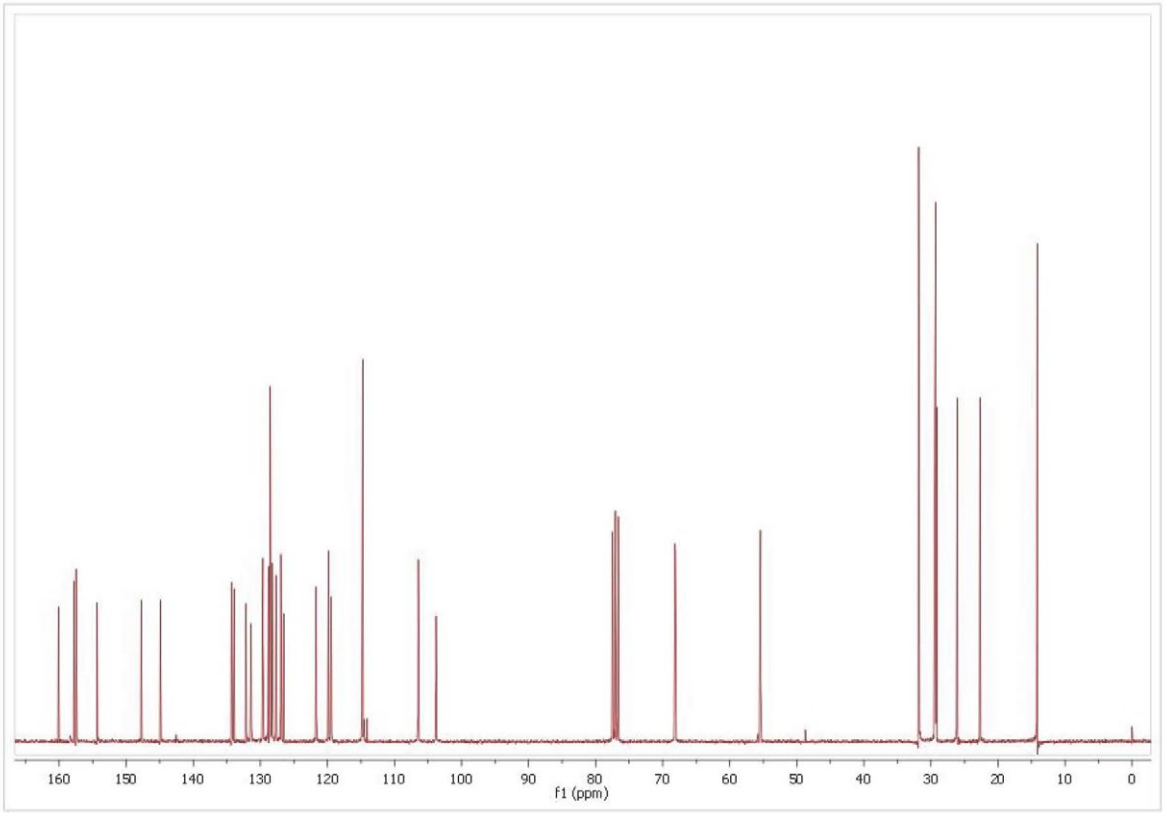

Figure S18. ^{13}C NMR (75 MHz, $CDCl_3$) spectra of compound **8d**.

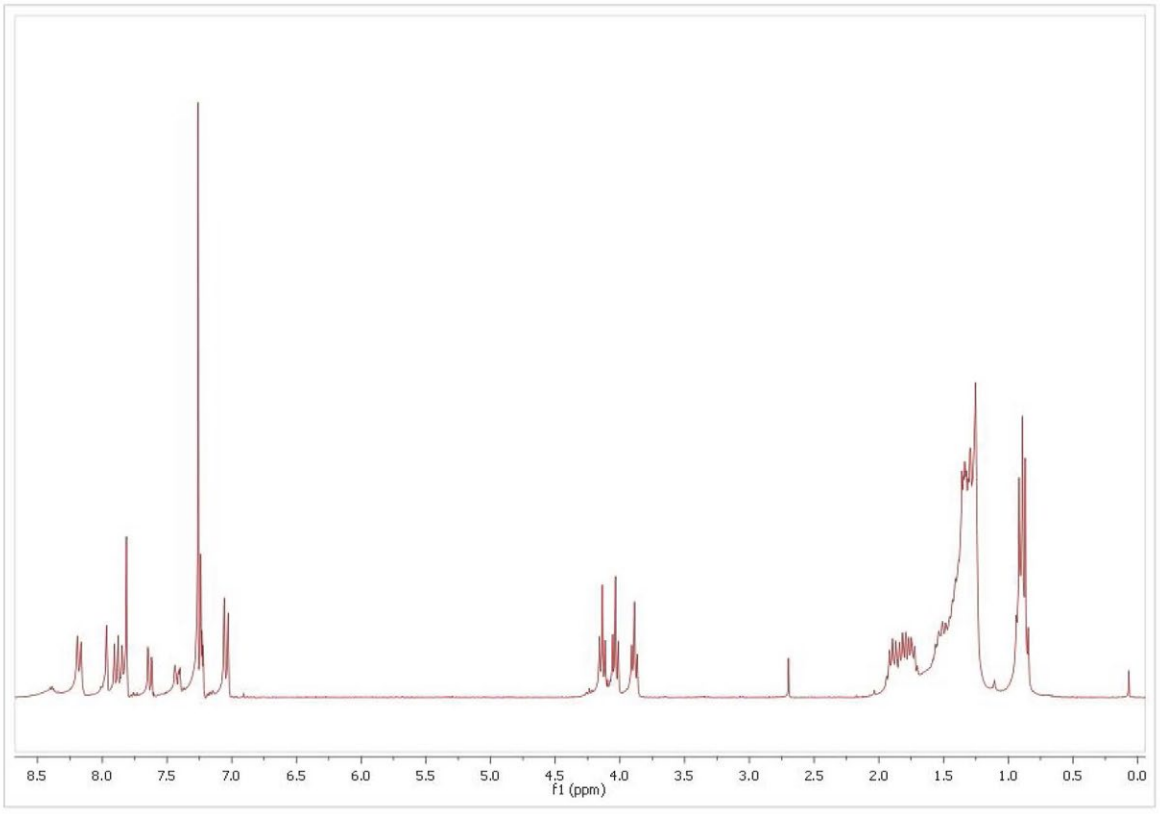

Figure S19. ^{1}H NMR (300 MHz, $CDCl_3$) spectra of compound **8e** (2.70 ppm, solvent peak).

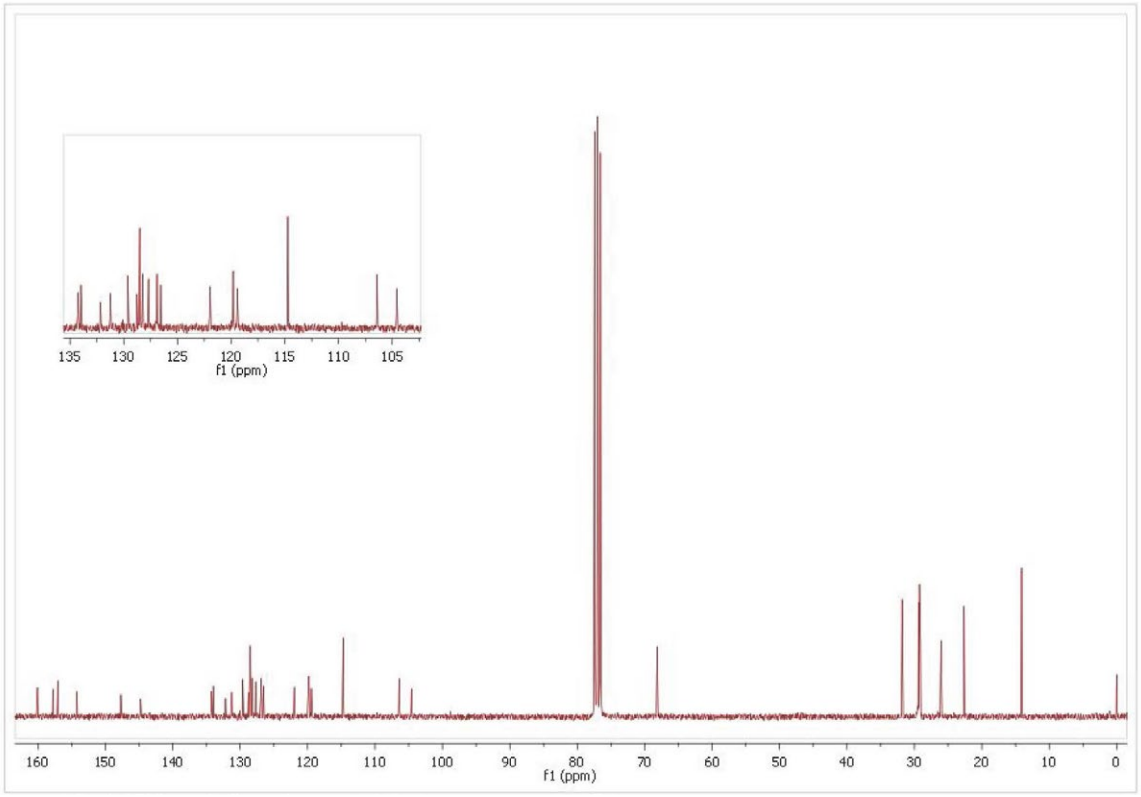

Figure S20. ^{13}C NMR (75 MHz, $CDCl_3$) spectra of compound **8e**.

Electrochemical studies

For estimation of the HOMO and LUMO, **8c** was selected and cyclic voltammetry experiments were carried out in Autolab PGSTAST, using a three compartment cell with a platinum shit as working electrode, Ag/AgCl electrode as reference and a Pt wire as counter electrode. The quinoline was measured using 0.1 mol L^{-1} $TBAPF_6$ in acetonitrile, as supporting electrolyte, at scan rate of 20 mV s^{-1}. The half-wave potential ($E^{1/2}$) of Fc/Fc^+ measured in 0.1 mol L^{-1} TBAPF acetonitrile solution is 0.41 V *vs.* Ag/AgCl.

Cyclic voltammetry results of quinoline **8c** were compared with UV-Vis data. Figure S1 shows the voltammetry curve in 0.1 mol L^{-1} of $TBAPF_6$. Figure S1 shows the oxidation and reduction peaks with values of 1.65 V and −0.55 V, respectively. The HOMO and LUMO energy levels were calculated using the oxidation and reduction values in equation 1.

$$E^{HOMO/LUMO} = [-e(E_{onset\ (vs..Ag/AgCl)} - E_{onset\ (Fc/Fc+\ vs..Ag/AgCl)}] - 4.8\ eV \quad (1)$$

Ferrocene potential at −4.8 eV was included to define the zero point. The HOMO energy was calculated as 6.06 (−eV) and the LUMO was 3.76 (−eV), therefore the energy gap from the electrochemical measurements were calculated as E_{gap} = 2.3 eV, which is in agreement with the E_{gap} obtained from the optical measurements as describe in the UV-Vis section. The band gap from UV-Vis spectra (1.98 eV) was obtained by extrapolation, using the equation $E_{gap} = 1240/\lambda$ (nm).

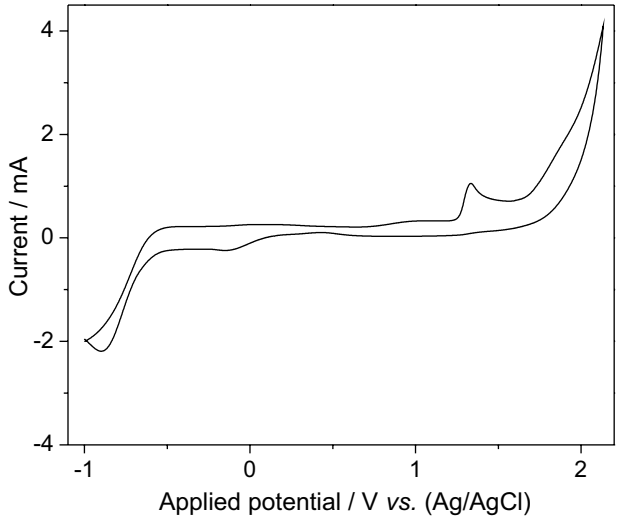

Figure S21. Cyclic voltammogram of the quinoline **8c** in 0.1 mol L^{-1} of $TBAPF_6$.

Spectral measurements

Absorption spectra were taken in a Thermo-scientific spectrometer using a 1 cm quartz cuvette. Steady-state fluorescence measurements were made in a HITACHI model F4500 spectrometer. Time-resolved fluorescence of the compounds were measured by time-correlated single-photon counting using a homemade picosecond spectrometer equipped with Glan-Laser polarizers (Newport), a Peltier-cooled PMTMCP (Hamamatsu R3809U-50) as the photon detector, and Tennelec-Oxford counting electronics. The light pulse was provided by frequency doubling the 200 fs laser pulse of a Mira 900 Ti-Sapphire laser pumped by a Verdi 5 W coherent laser, and the pulse frequency was reduced to 800 kHz using a Conoptics pulse picker. The fluorescence decays were excited at 400 nm and decay results were analyzed by a reconvolution procedure with instrument response function (irf). Fluorescence decay times were fitted with a bi-exponential function, optimizing Chi square, residuals, and standard deviation parameters. All solutions were deaerated by bubbling oxygen-free nitrogen. The mean fluorescence decay was calculated according to equation 2:

$$<\tau> = \frac{A_1\tau_1 + A_2\tau_2}{100} \quad (2)$$

where the τ_i is the individual decay time and A_i are the corresponding relative amplitudes. For fluorescence quantum yield experiments, the solutions were placed in 1 cm quartz cuvette and the absorbance of the compounds solutions was set at 0.1-0.2 to minimize inner-filter effects and the presence of aggregates. Transient absorption spectra were obtained using a LFP-112 Luzchem nanosecond laser flash photolysis spectrometer. Excitation of the samples was performed with the third harmonic (355 nm) of a Brio Nd-YAG laser, with 5.2 ns pulses. Kinetic analyses were made with the Luzchem proprietary software.

The fluorescence quantum yield at 293 K was obtained by comparison with the emission of anthracene in ethanol (Φ_F = 0.27).[1] The quantum yields were calculated according to equation 3:

$$\Phi_F = \frac{\int I(\lambda)\partial\lambda}{\int I(\lambda)^o\partial\lambda} \times \frac{DO_o}{DO} \times \frac{n^2}{n_o^2} \times \Phi_F^o \quad (3)$$

where the subscript "o" indicates the reference solution, DO is the optical density, Φ_F is the fluorescence quantum yield, $\int I(\lambda)$ is the integrated fluorescence intensity, and n is the refractive index of the solvent. The quantum yield at 77 K was calculated using equation 4:[2]

$$\Phi_F^{77K} = \frac{\int^{77K} I(\lambda)\partial\lambda}{\int^{293} I(\lambda)^0\partial\lambda} \times \Phi_F^{293K} \times f_c \quad (4)$$

where f_c is the solvent contraction constant (0.84) at 77 K, and $\int^{77K} I(\lambda)\partial\lambda$ and $\int^{293} I(\lambda)^0\partial\lambda$ are the areas of the fluorescence emission at 77K and 293 K, respectively.

Ground-state and excited singlet-state

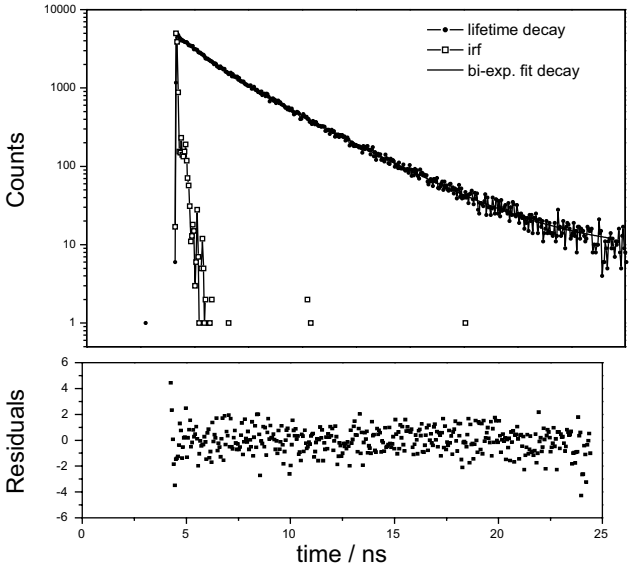

Figure S22. Fluorescence decay and residuals of quinoline **8d** following a bi-exponential fit decay. λ_{exc} = 400 nm and λ_{em} = 420 nm.

Exponential components analysis (reconvolution for fluorescence decay)

Fitting range: [87; 500] channels

χ^2: 1.066

decay	B_i	ΔB_i	f_i / %	Δf_i / %	t_i / ns	Δt_i / ns
1	0.2725	0.0313	25.464	3.882	1.174	0.044
2	0.3128	0.0157	74.536	3.866	2.994	0.005

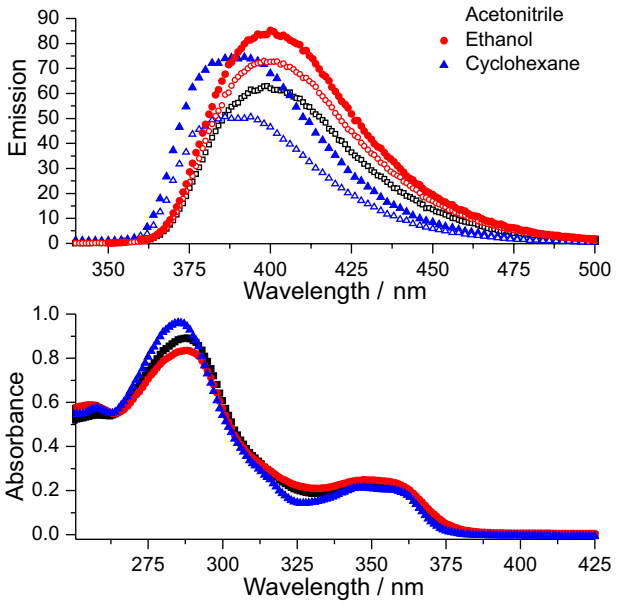

Figure S23. Absorption and emission spectra recorded to the quinoline **8b** in acetonitrile (■ black), ethanol (● red) and cyclohexane (▲ blue).

Crystallographic analysis

Crystallographic analysis was carried out with a single crystal Bruker APEX II DUO diffractometer using graphite-monochromated MoKα radiation (0.71073 Å) from a sealed tube operating at 1.5 kW and the temperature was set at 173 (± 2) K with an Oxford Instruments Cryojet system. Measurements were recorded by phi and omega scans with exposures of 30 s by frame using APEX2.[3] All collected data were corrected for Lorentz and polarization effects.[4] Due to very small absorption coefficient, no absorption correction was applied to the intensities. The structure was solved by direct methods and refined applying the full-matrix least-squares method using SIR97[5] and SHELXL97[6] software programs, respectively. All non-hydrogen atoms were refined with anisotropic displacement parameters. Hydrogen atoms were placed at their idealized positions with distances of 0.93 Å for C-H_{Ar}, 0.97 Å for C-H_2 and 0.96 Å for C-H_3 groups. The U_{iso} values for the hydrogen atoms were fixed at 1.2 times (for aromatic compounds and methylene) and 1.5 times (for methyl) the U_{eq} of the carrier atom (C). ORTEP plot of the molecular structure

Table S1. Solvent effect on the photophysical properties of **8e**

Solvent	λ_{MAX}^{abs} / nm		λ_{MAX}^{ems} / nm	λ_{ST} / nm	ε / (L mol^{-1} cm)	
	π-π*	n-π*			π-π*	n-π*
Acetonitrile	288	350	400	50	5.9×10^4	1.5×10^4
Ethanol	287	350	400	50	8.3×10^4	2.5×10^4
Cyclohexane	285	350	389	39	6.0×10^4	1.3×10^4

was produced with the PLATON program.[7] Further crystallographic information are shown in Table S2. Full tables containing the crystallographic data (except structure factors) have been deposited at the Cambridge Structural Database (CCDC 982481) and these data are available free of charge at www.ccdc.cam.ac.uk.

Table S2. Crystal data and structure refinement for **8e**

Empirical formula	$C_{49}H_{65}NO_3$
Formula weight	716.02
Temperature	173(2) K
Wavelength	0.71073 Å
Crystal system	Triclinic
Space group	Pī
Unit cell dimensions	a = 9.5071(3) Å b = 12.4764(4) Å c = 18.5693(6) Å α = 74.758(2)° β = 77.999(2)° γ = 84.217(2)°
Volume	2076.18(11) Å^3
Z	2
Density (calculated)	1.145 mg m^{-3}
Absorption coefficient	0.069 mm^{-1}
F(000)	780
Crystal size	0.40 × 0.20 × 0.04 mm^3
Theta range for data collection	1.69 to 28.00°
Index ranges	$-12 \leq h \leq 11$, $-16 \leq k \leq 16$, $-24 \leq l \leq 24$
Reflections collected	26902
Independent reflections	10036 (R_{int} = 0.0179)
Refinement method	Full-matrix least-squares on F^2
Data/restraints/parameters	10036/0/481
Goodness-of-fit on F^2	1.043
Final R indices [I > 2sigma(I)]	R1 = 0.0483, wR2 = 0.1351
R indices (all data)	R1 = 0.0623, wR2 = 0.1471
Largest diff. peak and hole	0.388 and −0.223 e Å^{-3}

References

1. Berlman, I. B.; *Handbook of Fluorescence Spectra of Aromatic Molecules,* Academic Press: New York, 1971; Dawson, W. R.; Windsor, M. W.; *J. Phys. Chem.* **1968**, *72*, 3251.
2. Biczók, L.; Bérces, T.; Linschitz, H.; *J. Am. Chem. Soc*. **1997**, *119*, 11071; Leigh, W. J.; Lathioor, E. C.; Pierre, M. J. S.; *J. Am. Chem. Soc.* **1996**, *118*, 12339.
3. *APEX II*, *Data Collection Software*, version 2011.8-0; Bruker AXS Inc.: Madison, WI, 2005-2011.
4. Bruker APEX2, SAINT, Bruker AXS Inc., Madison, Wisconsin, USA, 2009.
5. Altomare, A.; Burla, M. C.; Camalli, M.; Cascarano, G. L.; Giacovazzo, C.; Guagliardi, A.; Moliterni, A. G. G.; Polidori, G.; Spagna, R.; *J. Appl. Crystallogr.* **1999***, 32*, 115.
6. Sheldrick, G. M.; *Acta Crystallogr.* **2008**, *A64*, 112.
7. Spek, A. L.; *J. Appl. Crystallogr.* **2003**, *36*, 7; Bruno, I. J.; Cole, J. C.; Edgington, P. R.; Kessler, M. K.; Macrae, C. F.; McCabe, P.; Pearson, J.; Taylor, R.; *Acta Crystallogr*. **2002**, *B58*, 389.